January 2014

Evaluation Of Selected Spectral Vegetation Indices In Senescent Rangeland Canopy Using Landsat Imagery

Marla Collins

EVALUATION OF SELECTED SPECTRAL VEGETATION INDICES IN SENESCENT RANGELAND CANOPY USING LANDSAT IMAGERY

by

Marla Striped Face-Collins
Bachelor of Science, Sitting Bull College, 2008

A Thesis
Submitted to the Graduate Faculty

of the

University of North Dakota

in partial fulfillment of the requirements

for the degree of

Master of Science

Grand Forks, North Dakota
May
2014

This thesis, submitted by Marla Striped Face-Collins in partial fulfillment of the requirements for the Degree of Master of Science from the University of North Dakota, has been read by the Faculty Advisory Committee under whom the work has been done and is hereby approved.

_____
Bradley C. Rundquist

_____
Paul E. Todhunter

_____
Rebecca L. Phillips

This thesis is being submitted by the appointed advisory committee as having met all of the requirements of the School of Graduate Studies at the University of North Dakota and is hereby approved.

_____
Wayne Swisher
Dean of the School of Graduate Studies

_____
Date

PERMISSION

Title Evaluation of Selected Spectral Vegetation Indices in Senescent Rangeland Canopy Using Landsat Imagery

Department Geography

Degree Master of Science

In presenting this thesis in partial fulfillment of the requirements for a graduate degree from the University of North Dakota, I agree that the library of this University shall make it freely available for inspection. I further agree that permission for extensive copying for scholarly purposes may be granted by the professor who supervised my thesis work or, in his absence, by the Chairperson of the department or the dean of the School of Graduate Studies. It is understood that any copying or publication or other use of this thesis or part thereof for financial gain shall not be allowed without my written permission. It is also understood that due recognition shall be given to me and to the University of North Dakota in any scholarly use which may be made of any material in my thesis.

Marla Striped Face-Collins
May 2014

TABLE OF CONTENTS

LIST OF FIGURES

Figure Page

LIST OF TABLES

Table Page

ACKNOWLEDGMENTS

I was an intern at the USDA Agriculture Research Station in Mandan, ND, and assisted in gathering the field data at the 72 sites for this project in summer 2010. This research paper is made possible through the help and support from my advisor, committee members, and family. I am grateful and I especially want to acknowledge the following significant advisors and contributors: First and foremost, I would like to thank Dr. Rebecca Phillips for her contribution to my thesis and for the support and encouragement she has given. Second, I would like to thank Dr. Bradley Rundquist, who not only provided valuable advice but read my thesis and provided valuable and constructive feedback. Thirdly, the work would not have been possible without the kind cooperation of the Dakota Prairie Grasslands' managers (Phil Sjursen, Dan Svingen, the staff at the Lemmon, South Dakota field office) and the GRNG ranchers. I appreciate John Henrickson and Mary Kay Tokach for sharing the knowledge they have on plants and for their assistance in plant identification. I want to thank the team members, Moffatt Ngugi, Nicanor Saliendra, Justin Feld, Sarah Waldron, and Cari Ficken for their work, as well as Mark West for assisting with the data statistics.

Finally, I sincerely thank my husband, E. Michael Collins, my family and friends for providing advice and support and special "Thank you" to my friend, Stacy Hazen, for her support that was really needed and much appreciated.

The production of this thesis would not been possible without all of them.

ABSTRACT

Grassland birds are diminishing more steadily and rapidly than other North American birds in general. The nesting success of some grassland bird species depends on the amount of nonproductive vegetation (NPV). To estimate NPV land managers are currently using the Robel pole visual obstruction reading methods. Researchers with the USDA Agricultural Research Service's (ARS) Northern Great Plains Research Laboratory in Mandan, ND, recently established statistical relationships between photosynthetic vegetation (PV), NPV and spectral vegetation indices (SVIs) derived from more sensitive and more detailed, but less accessible and more costly hyperspectral aerial imagery. This study is an extension of this previous work using spectral vegetation indices collected using the Landsat TM sensor, including simple ratios SWIR-SR (ρ_{2215}/ρ_{1650}) and SR71 (ρ_{2215}/ρ_{485}) to estimate the amount of NPV and bare ground cover, respectively.

CHAPTER I

INTRODUCTION

Background

Senescent grassland canopy structure is vital for nesting and predation cover for many avian species (Larvière 2003), some of which are rare or endangered. Senescent grasses are also critical because they provide the bulk of the winter feed for wildlife and livestock (Marsett et al. 2006). Livestock and grassland birds benefit from diverse mosaics of grassland habitat through the management of cattle grazing (U.S. Department of the Interior 2013).

Avian Habitat

Long-term sustainable grazing systems yield better food resources for livestock as well as healthier habitats for grassland and arid land birds (U.S. Department of the Interior 2013). Grassland bird populations are declining faster and more consistently than any other group of North American birds (Samson and Knopf 1994, Herkert 1995). Some grassland bird species have habitat requirements for short grasses with heavy disturbance; others require undisturbed, thick patches of taller grasses (U.S. Department of the Interior 2013).

For example, the nesting success of the clay-colored sparrow (*Spizella pallida*) increased with increasing percentage of nest cover by vegetation and vegetation height from

the surrounding vegetation (Winter et al. 2005). The occurrence of the western meadowlark (*Sturnella neglecta*) and the clay-colored sparrow is clearly associated with litter depth (Bakker et al. 2002). Intensely grazed areas are preferred by the mountain plover (*Charadrius montanus*) and McCown's longspur (*Rhynchophanes mccownii*) while other areas that are lightly grazed or untouched are favored by the bobolink (*Dolichonyx oryzivorus*) and the upland sandpiper (*Bartramia longicauda*) (U.S. Department. of the Interior 2013).

Bare ground could have an effect on the density of some species such as the mountain plover, also known as the prairie plover or the upland sandpiper. The plover have adapted to sparsely vegetated and bare ground areas for nesting that is associated with various disturbances such as heavy grazing, prairie dog colonies and recently burned short-grass prairie (NRCS 2001; U.S. Department of the Interior 2013). Although the plover's essential habitat feature is bare ground they will tolerate up to 70 percent short vegetation ground cover (NRCS 2001).

Senescent Biomass Assessment

To assess the amount of senescent vegetation available for grassland bird habitat, the USDA Forest Service currently uses the Robel pole method. Robel et al. (1970) developed a transect method that uses a special pole that allows technicians and researchers to quickly make measurements of visual obstruction (VO) as a surrogate measure of above ground biomass, which otherwise would require the labor-intensive and time-consuming alternative method of grassland clipping, transport, and weighing. Robel et al. (1970) found that VO measurements taken at a height of 1 m and a distance of 4 m from the pole gave a reliable

estimate of the amount of above-ground vegetation production at a given location. A few of the drawbacks to using the Robel pole are: 1) the training phase is omitted or skipped where the users compare estimates to clipped vegetation measurements; and 2) ocular estimates vary among users (Schultz et al. 1961, Kershaw 1973, Block et al. 1987, Irving et al. 1995).

Another perhaps more beneficial and complementary approach to assess grassland canopy biomass non-destructively is through the use of remote sensing (via the reflectance spectra of ground objects at diverse resolutions), which can be made over very large geographic areas in a timely fashion.

A complex mixture of photosynthetic vegetation (PV), non-photosynthetic vegetation (NPV) (Huete and Escadafal 1985, van Leeuwen and Huete 1996), plant form, soil (%BG; Huete 1988), and shadow (Curran 1983) contributes to grassland canopy spectral response (Rundquist 2002). Typically, PV is the canopy characteristic that is the focus of remote sensing studies of grasslands (Marsett et al. 2006). Remote sensing of NPV has been neglected because many researchers have presented and/or suggested that various canopy features such as plant architecture and soil background are the prevailing sources of deviation between field and remote sensing measurements (Elvidge and Lyon 1985, Huete and Escadafal 1985, Huete and Tucker 1991, Todd and Hoffer 1998). However, scientists and land managers recognize the importance of estimating canopy characteristics for mixtures of both PV and NPV because of their importance in ecosystem models that estimate rates of carbon and nutrient uptake, the exchange of latent and sensible heat between the surface and atmosphere, and surface albedo (Guerschman et al. 2009). They reported that the simple ratio (ρ_{2130}/ρ_{1640}) was an optimum vegetation index for estimating NPV fractional cover when applied to MODIS spectral data (Guerschman et al. 2009). In addition, NPV cover is vital in

predicting fire frequency and intensity and the rates of wind and water erosion (McTainsh et al. 2006). The amount of NPV is also important in ensuring the nesting success of some species of grassland birds (Marsett et al. 2006).

Accumulation of NPV in a canopy has a non-linear impact on overall canopy reflectance, and thus, accurately estimating its amount using remote sensing-based methods is a challenge (Asner 1998, Zhang et al. 2011). For example, other researchers have shown that plant physiological processes associated with regrowth following defoliation is the dominant influence on spectral response early in the growing season, while the accumulation of senescent material dominates during the latter half, with small increases in the percentage of senescent vegetation having disproportionally large effects on overall reflectance (Marsett et al. 2006).

Research Questions and Objectives

The question this research seeks to answer is: "Can the biomass of senescent vegetation in a grassland canopy be accurately estimated at Grand River National Grassland (GRNG) using Landsat Thematic Mapper (TM) imagery?"

I anticipate spectral vegetation indices (SVIs) will vary with respect to senescent biomass estimation. Those SVIs that use middle-infrared energy bands (TM Bands 5 and 7) should be more effective for senescent biomass detection (Tucker 1979, Huete et al. 1997, Guerschman et al. 2009). To determine the most effective SVI, several known SVIs will be compared with data collected at field plots. The ultimate goal of this research is to develop a model that conceivably could be extrapolated to the landscape scale for use by rangeland managers, research scientists, and others.

Although multispectral instruments such as the Landsat TM convolve large, noncontiguous regions of the spectrum into broad bands and thus a single number represents the radiometric dynamics of a large region of the spectrum (Asner 1998), making narrow-band analysis difficult, this study seeks to assess the applicability of using Landsat TM imagery and derived SVIs to estimate the amount of NPV cover late in the growing season at the GRNG, located in northwestern South Dakota and managed by the USDA Forest Service. This study proposes to extend previously published studies, where statistical relationships between PV, NPV and SVIs were derived using hyperspectral aerial imagery (Phillips et al. 2013). Modeled field data and aerial hyperspectral imagery effectively predicted post-growing season canopy attributes in mixed grass prairie landscapes (Phillips et al. 2013). Using a resampling VI model procedure, the simple ratio of short-wave infrared and red band data, SWIR-SR (ρ_{2128}/ρ_{1642}), was found to be the single most predictive VI of TSC and NPV, with generally greater values of TSC and NPV at lower values of SWIR-SR. Researchers are interested in investigating the validity of these findings using the broad-band, moderate resolution Landsat TM, ETM+, and OLI because of its relative ease of access, multi-temporal availability (30+ years, 8-day frequency) and lower cost (now offered free by the USGS).

Study Area

The Grand River National Grassland (GRNG) is located in northwestern South Dakota (45.7˚ N, 102.5˚W) comprising approximately 61,108 hectares in three counties – Perkins, Corson and Ziebach (Omernik 1987; Fig. 1).

Figure 1. State of South Dakota. Grand River National Grassland in the northwest part of South Dakota.

The annual precipitation at the GRNG during the growing season is about 35 cm. The average monthly temperature ranges from a high of 21˚C in July to a low of -9˚C in January. Elevation range is 670-880 m with open plains to rolling grassland hills (Fig. 2).

The GRNG is intermingled with private lands; therefore, it is not contiguous (Hansen 2008). This mixed-grass prairie ecosystem is characterized by the presence of blue grama (*Bouteloua gracilis*) and western wheatgrass (*Pascopyron smithii).* A considerable amount of the GRNG lowlands were formerly cultivated creating present-day stands of crested wheatgrass (*Agropyron cristatum*) (Sjursen 2009).

According to the U.S. Forest Service (USFS) Land and Resource Management Plan's guidelines (2001), mowing of grasslands for winter hay is delayed until July 15 or later to protect ground-nesting birds, including their nests and young broods, and livestock turn-on

dates are delayed until June 15 or later in areas grazed in the previous grazing season to provide quality nesting cover. Therefore, the managers of GRNG strive to conserve a plant canopy height of approximately 9 cm to ensure adequate cover the following spring for avian nesting concealment, but the GRNG is seasonally grazed from May to October by cattle (stocking rate is approximately one animal unit per hectare). The Management Plan prohibits prescribed burning in any areas known to support wintering or nesting populations.

Reported correlations between biomass and visual obstruction readings during the growing season may be representative when vegetation is senescent. Management decisions based on readings obtained in autumn are contended by ranchers who believe VOR data may not represent biomass accurately. In October, loss of plant turgor pressure and high winds might cause grasses to lay down that would typically be upright in July (Phillips 2014, personal communication).

Figure 2. Grand River National Grassland. (Photo courtesy of Dr. Rebecca Phillips)

CHAPTER II

DATA AND METHODS

The study area and sample design were previously described (Phillips et al. 2012) and are briefly summarized here. The Grand River National Grassland land-cover includes a mixture of herbaceous and non-herbaceous vegetation, roads, rivers, and buildings. Herbaceous land-cover was the target, so an object-based classification method was used on a Landsat 5 TM image (acquired July 10, 2008) to map herbaceous grassland only at the GRNG. This involved segmenting six TM bands in Definiens eCognition Developer (v.7) ® object-based classification software (Benz et al. 2004). Binary recursive classification and regression tree algorithm (Feldesman 2002, Phillips et al. 2012) implemented in the R® statistical package (R Development Core Team 2009) was used to classify the image objects (based on their spectral characteristics) into herbaceous and non-herbaceous vegetation classes (Bittencourt and Clarke 2003, Phillips et al. 2012). Only areas classified as herbaceous vegetation cover on federally managed land were retained for field sampling and future analysis (Phillips et al. 2012). These classification results yielded a USFS grassland area of 36,000 ha, which was used in all subsequent analyses (Fig. 3) and is herein referred to as our landscape-of-interest (LOI). The goal was to randomly select sample plots within the herbaceous vegetation classification to include the full range of spatiotemporal variability in aboveground production for an area of this size. To ensure that inherently low, medium and

high production areas were included, the landscape was evaluated for spatial trends in vegetation greenness using 10 years of spectral data (see below).

Moderate Resolution Imaging Spectrometer (MODIS) data were downloaded from the MODIS global subsets website (http://daac.ornl.gov/MODIS/modis.shtml). Specifically, the 16-day Enhanced Vegetation Index (EVI; Huete et al. 1997) was calculated using MODIS imagery collected in June and July from 2000 to 2009. A total of 40 images were combined into one multi-temporal band image, and an unsupervised classification was performed using ENVI/IDL® to identify those areas where EVI was consistently higher or lower than surrounding areas over the 10-year period. The unsupervised classification identified five spectral categories in the landscape where EVI values tended to be higher or lower during June and July. Four of these categories represented 21, 22, 26, and 29 percent of the LOI and were mapped respectively (Fig. 3) and referred to as historical reflectance indices (HRI). Areas shown in red (low HRI) were historically lower in EVI than blue (med-low HRI), yellow (med-high HRI), and green (high HRI) areas. Since Phillips et al. (2012) found the four HRI classes comprised 98% of the landscape, the fifth was not considered further. Stratification of the herbaceous landscape into these four landscape categories facilitated collection of field data representing a range of vegetation greenness for the LOI (Fig. 3).

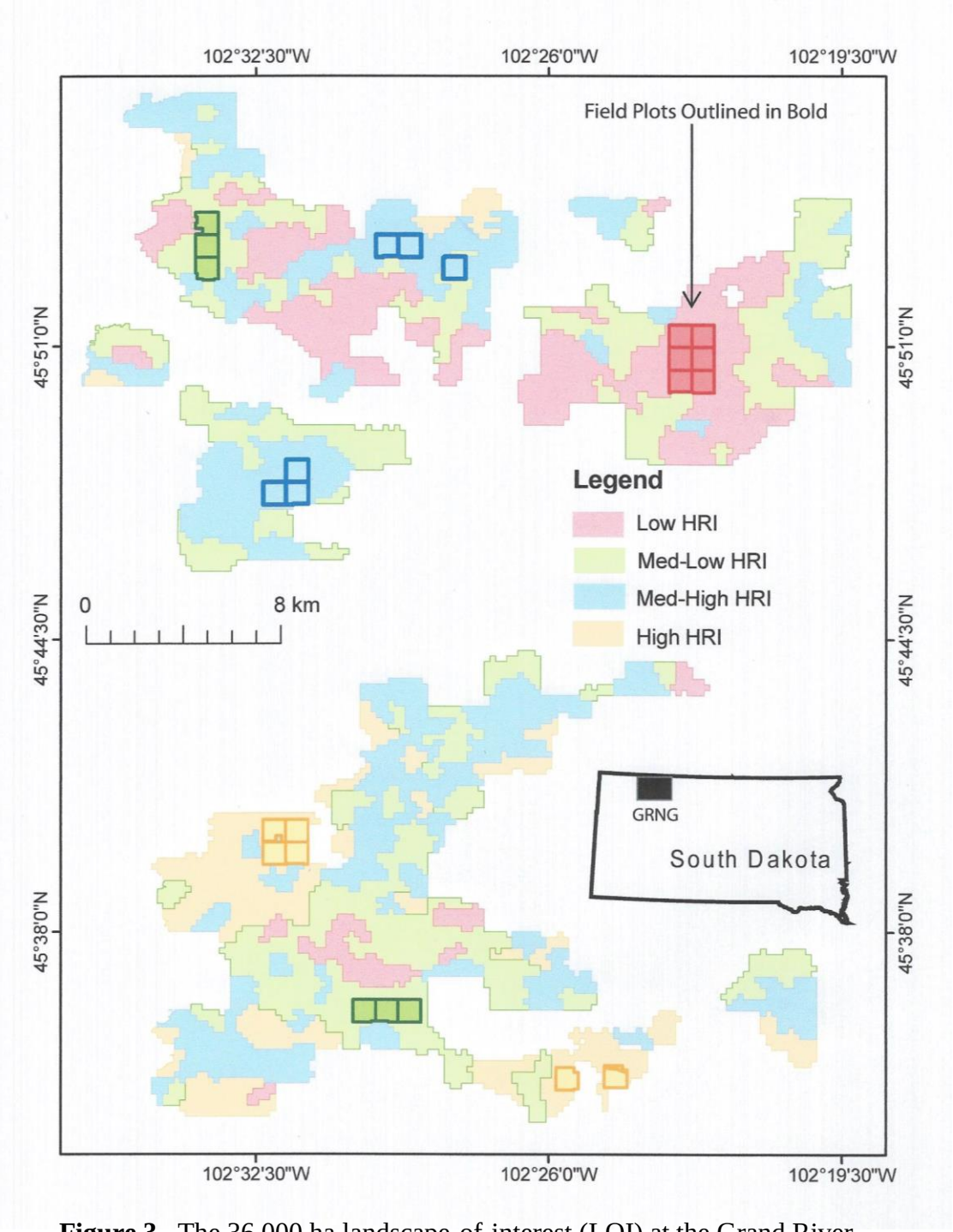

Figure 3. The 36,000 ha landscape-of-interest (LOI) at the Grand River National Grassland near Lemmon, South Dakota. The four categories of herbaceous vegetation were based on an unsupervised classification of MODIS EVI 10-yr data set. Locations of field plots are outlined in bold (Phillips et al. 2012).

Plot Selection and Field Data Collection

Six random field plots were selected within each of the four color-coded landscape HRI classes identified by the 10-year unsupervised classification (Fig. 3) using 1-km MODIS pixels. Potential sample plot pixels were selected to be homogenous (no mixed pixels) and were located to represent summit, midslope and toeslope locations. These random points (MODIS pixel centers) were generated in ESRI ArcGIS (Environmental Systems Research Institute, Redlands, CA) and geo-located in the field (Dauwalter et al. 2006) using a sub-meter, real-time, differential Trimble Geo XT Global Positioning System (GPS) and Beacon receiver (Trimble Navigation, Sunnyvale, CA). The ARS researchers found points that were not safely accessible with an all-terrain vehicle, and those were removed and replaced with new points to achieve a total of six field-plots per category (Fig. 3). Locations of field plots are outlined in bold. Phillips et al. (2012) found accessibility was particularly problematic for the six plots bordering each other in Category 3 (see Figs. 3 and 26). The range of elevations recorded at field sites was 740-850 m. Each position was flagged for subsequent sample collection (Fig. 3). The researchers selected the nearest south facing slopes to minimize any effects of aspect and sun exposure variation on plant properties examined, so that observed difference in sampling locations could be attributed to topographic position and not aspect (Milchunas et al. 1989, Phillips et al. 2012).

Each point was precisely geo-located (<1 m spatial resolution) using a Global Positioning System (Trimble Geo XT; Fig.4).

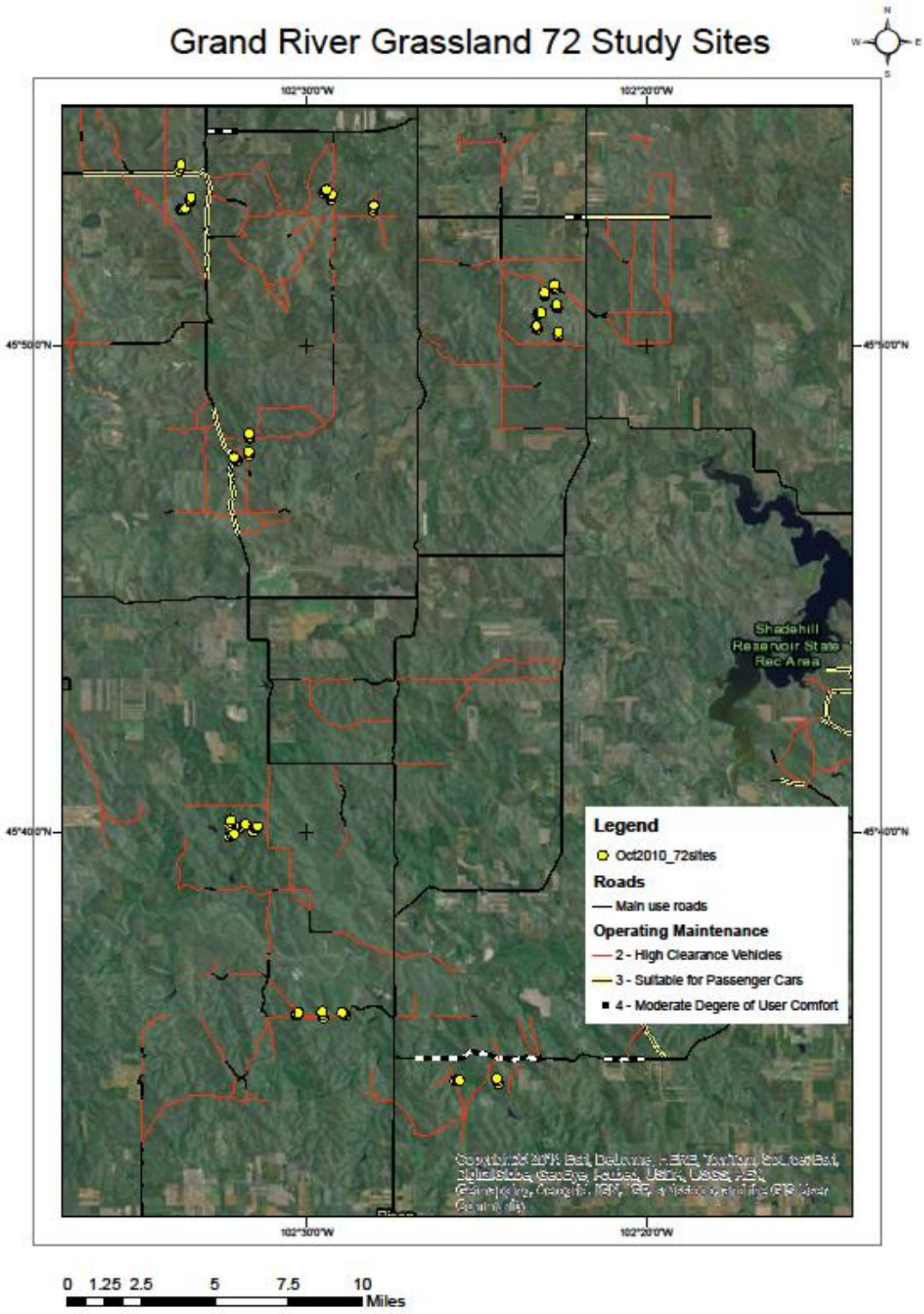

Figure 4. Grand River Grasslands 72 study sites located in the Northwest Region of South Dakota.

Vegetation and rock/bare soil were characterized as percent cover at each of the 72 sites (24 plots x three positions) between 20 June and 15 July 2010, using Daubenmire frames (Daubenmire 1959). Frames (0.5 x 0.2 m) were placed both 1 and 2 m from the center of the plot in the cardinal directions (Fig. 5). This resulted in a total of eight frames per site. Daubenmire frames provide a method to visually estimate percent cover using a predetermined set of estimate ranges. Phillips et al. (2012) estimated species cover within each frame as either <5%, 5-25%, 25-50%, 50-75%, or greater than 75%. Minor species representing <5% of plant cover that could not be identified were logged as unknown vegetation. All species representing more than 5% of the canopy were identified and average species cover calculated using all eight frames at each site.

Each species was assigned to forb, mid-grass or short-grass functional groups. Rocks and bare ground were assigned to a non-vegetation group and senescent vegetation was assigned to the litter group. Dominant and co-dominant species based on percent cover were identified for (a) the four frames closest to center and (b) the four frames furthest from the center of the plot. All vegetation within the frame was clipped to 2 cm above the soil surface, separated it into PV and NPV groups, then dried the vegetation for 48 hours at 60°C. Total standing crop biomass was calculated (TSC, kg ha^{-1}) as the sum of PV and NPV. Water content was calculated based on percentage of water lost between field-moist and dried plant samples. The vegetation for PV was ground separately from NPV through a 1-mm mesh screen, and analyzed for total N using dry combustion on a Carlo Erba Model NA 1500 Series 2N/C/S analyzer (CE Elantech, Lakewood, NJ). Canopy N content (kg N ha^{-1}) was calculated using N content and mass for both PV and NPV vegetation. Average PV,

NPV, TSC, Canopy N, and percent vegetation cover by point were used in all subsequent analyses (Phillips et al. 2012, Phillips et al. 2013).

The Robel pole (Robel et al. 1970, Uresk and Benson 2007) was used to measure vegetation height at each of the 72 sites (24 plots x three positions; Phillips et al. 2012). The height was measured 3 m from center in each of the four cardinal directions (Fig. 4).

As previously reported in Phillips et al. (2012), consistent trends in species cover by topographic position groups were identified, where mid- and toe slopes were dominated by mid-grass species and summits were dominated by short-grass species. Phillips et al. (2013) found that the October canopy data attributes varied significantly from the July data with topographic position (Phillips et al. 2012). The three attributes TSC, NPV, and % bare ground for October were ($F_{2,40} = 18.05$; $p < 0.0001$); ($F_{2,40} = 15.24$; $p < 0.0001$); and ($F_{2,40} = 23.78$; $p < 0.0001$), respectively, and the TSC and canopy height data analysis resulted in an $R^2 = 0.62$ (Phillips et al. 2013).

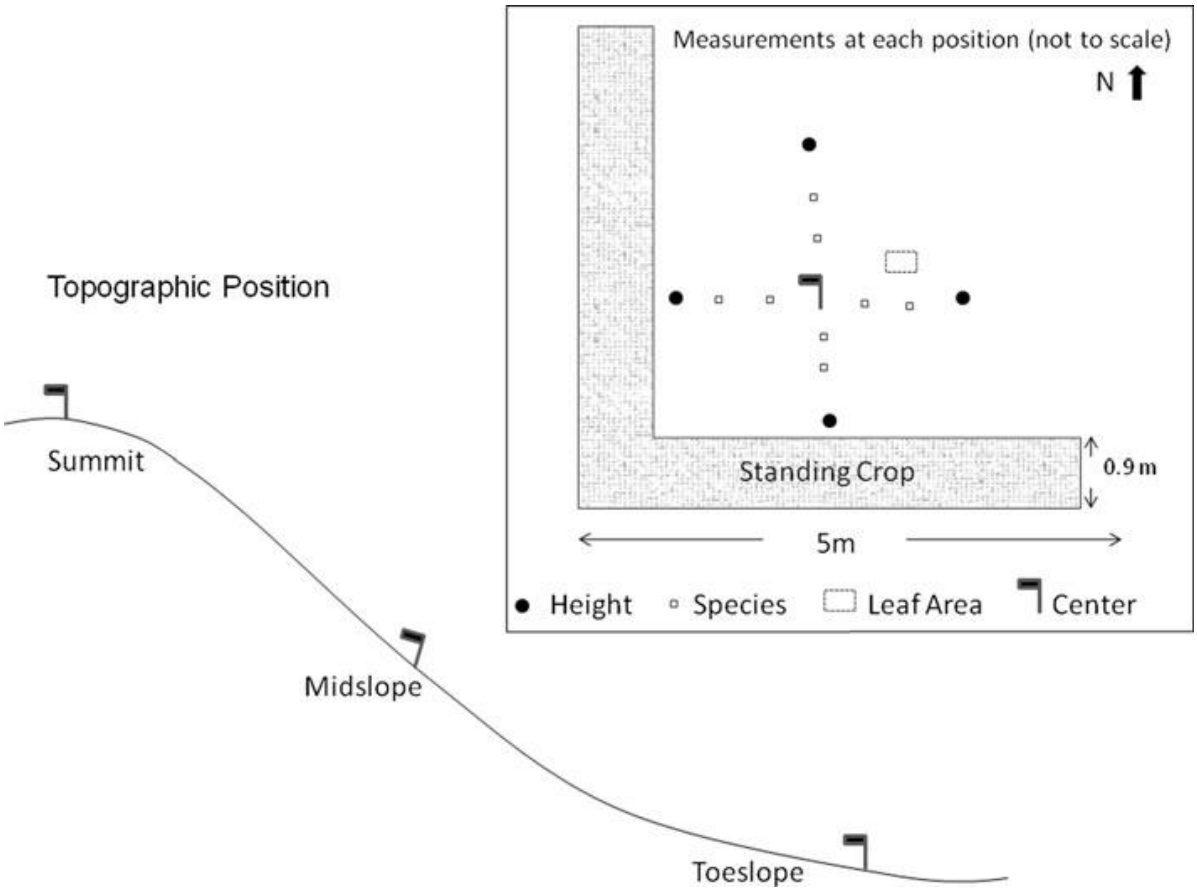

Figure 5. The field sampling design for collection of vegetation attributes associated with canopy structure. At each field plot, aboveground vegetation data were collected according to the figure inset at summit, midslope and toeslope positions (Phillips et al. 2012).

Data Processing and Statistical Analyses

The same field plot data sets collected, described in detail and reported in previous work (Phillips et al. 2012 and Phillips et al. 2013) are used in this study. Cloud-free georeferenced Landsat 5 TM imagery from 20 October 2010, was selected to correspond to post grazing senescent grass conditions similar to that used in Phillips et al. (2013). During the various steps of Landsat data processing band designations changed from Fast Line-of-sight Atmospheric Analysis of Spectral Hypercubes (FLAASH) Bands 0, 1, 2, 3, 4, and 5 to Landsat TM Bands 1, 2, 3, 4, 5, and 7 (Table 1, personal communication email 09-09-11). FLAASH is an atmospheric correction tool within the image processing software ENVI (Environment for Visualizing Images; Excelis Visual Information Solutions, Research Systems, Inc., Boulder, CO).

Table 1 Landsat data processing band designations in FLAASH Bands to Landsat TM Bands.

Wavelength (nm)	FLAASH_Band	Landsat-TM_Band
485	0	1
560	1	2
660	2	3
830	3	4
1650	4	5
2215	5	7

Note: The thermal Band 6 I the Landsat-TM is excluded in the FLAASH reflectance output.

Field Data Analyses

These field results from Phillips et al. (2013) are used in this study as input data into the evaluation of Landsat TM imagery as a potentially valid basis for adaptive grassland management using remote sensing.

SAS (SAS System for Windows, copyright© 2002-2008, SAS Institute Inc., Cary, NC) software was used to identify the SVI most predictive for each variables here. Included in the model selection procedure were the list of SVIs (listed below 1-5) and vegetation water content. The model used 2/3 of the data to selected predictive variables and 1/3 of the data to validate results and calculate R^2.

Model Selection

Topographic position was an important factor in TSC and NPV predictive models, particularly summits. As such, separate equations were required to predict TSC and NPV at summits, compared to midslopes and toeslopes (equations listed below):

1) Summit TSC, or Total_kg_ha^{-1} = 6720+ (-5153*SWIR-SR_LS)+(% water content * 25.5) - 548, R^2 = 0.55
2) Midslope and Toeslope TSC, or Total_kg_ha^{-1} = 6720+ (-5153*SWIR32_LS)+(% water content * 25.5), R^2 = 0.55
3) Summit NPV_kg_ha^{-1} = 2593+ (-1686*SWIR-SR_LS) + (% water content * -13) -266, R^2 = 0.54
4) Midslope and Toeslope NPV_kg_ha^{-1} = 2593+ (-1686*SWIR-SR_LS) + (% water content * -13), R^2 = 0.54

5) Summit, Midslope, Toeslope, %BG = 227+(-9*SR71) +(-640*SWIR-SR)+ (0.37* %water content) + (480.6*SWIR-SR*SWIR-SR), $R^2 = 0.63$

Although five similar models developed using Partial Least Squares Regression (PLSR) are discussed in previous work (Phillips et al. 2013), only the first three (TSC, NPV, %BG) were considered critical in assessing senescent grassland canopy structure as it relates to avian habitat. Similar to results for AVIRIS hyperspectral data collected at these field sites October 20, 2010, the Landsat TM SWIR-SR was the single most predictive SVI for TSC, NPV and %BG.

Table 2. a) Vegetation Indices (VIs) calculated from reflectance data derived from b) Landsat-TM spectral bands.

a) Vegetation Index	Equation	Reference
EVI, Enhanced Vegetation Index	$2.5*(\rho_{830} - \rho_{660}) / (\rho_{830} + 6* \rho_{660} - 7.5*\rho_{485} + 1)$	Huete et al. 1997
NDVI, Normalized Difference Vegetation Index	$(\rho_{830} - \rho_{660}) / (\rho_{830} + \rho_{660})$	Tucker 1979
Simple Ratio SR71	ρ_{2215} / ρ_{485}	
Simple Ratio SWIR-SR	$\rho_{2215} / \rho_{1650}$	Guerschman et al. 2009
SWIRDVI, SWIR Difference Vegetation Index	$(\rho_{1650} - \rho_{2215}) / (\rho_{1650} + \rho_{2215})$	
b) Landsat-TM	Wavelength (nanometers)	Midpoint (nanometers)
Band 1	450 – 520; visible, blue	485
Band 2	520 – 600; visible, green	560
Band 3	630 – 690; visible, red	660
Band 4	760 – 900; near infrared (NIR)	830
Band 5	1,550 - 1,750; short wave infrared (SWIR2)	1,650
Band 7	2,080 - 2,350; short wave infrared (SWIR3)	2,215
Band 6	10,400 – 12,500; thermal	11,450

CHAPTER III

RESULTS

Field Data

As noted in the prior work at this LOI, above-ground vegetation attributes (TSC and NPV increasing) and %BG (decreasing) varied significantly with decreasing topographic elevation. Data point distributions for the three topographic positions, summit (red), midslope and toeslope (green) (Figs. 5 through 18) illustrate this relationship. Midslope and toeslope were combined into one color category (green) because of similarities in vegetation type and data values distribution.

Total Standing Crop (TSC)

Total standing crop clippings for 72 sites yielded estimates ranging from 127 to 4,380 kg ha $^{-1}$ with a mean of 1,580 kg ha $^{-1}$.

The correlation between TSC from clippings data and Robel pole measurements was significant with a correlation coefficient (R) of 0.79 (Fig. 6). The relation of TSC to topographic position is less pronounced (as TSC increases, canopy height increases).

These positive results and subsequent consistent statistical correlations are attributed in large part to the skills and experience of the field technicians who collected the data. This

may not always be the case in rangeland management assessments as noted by Limb et al. (2007).

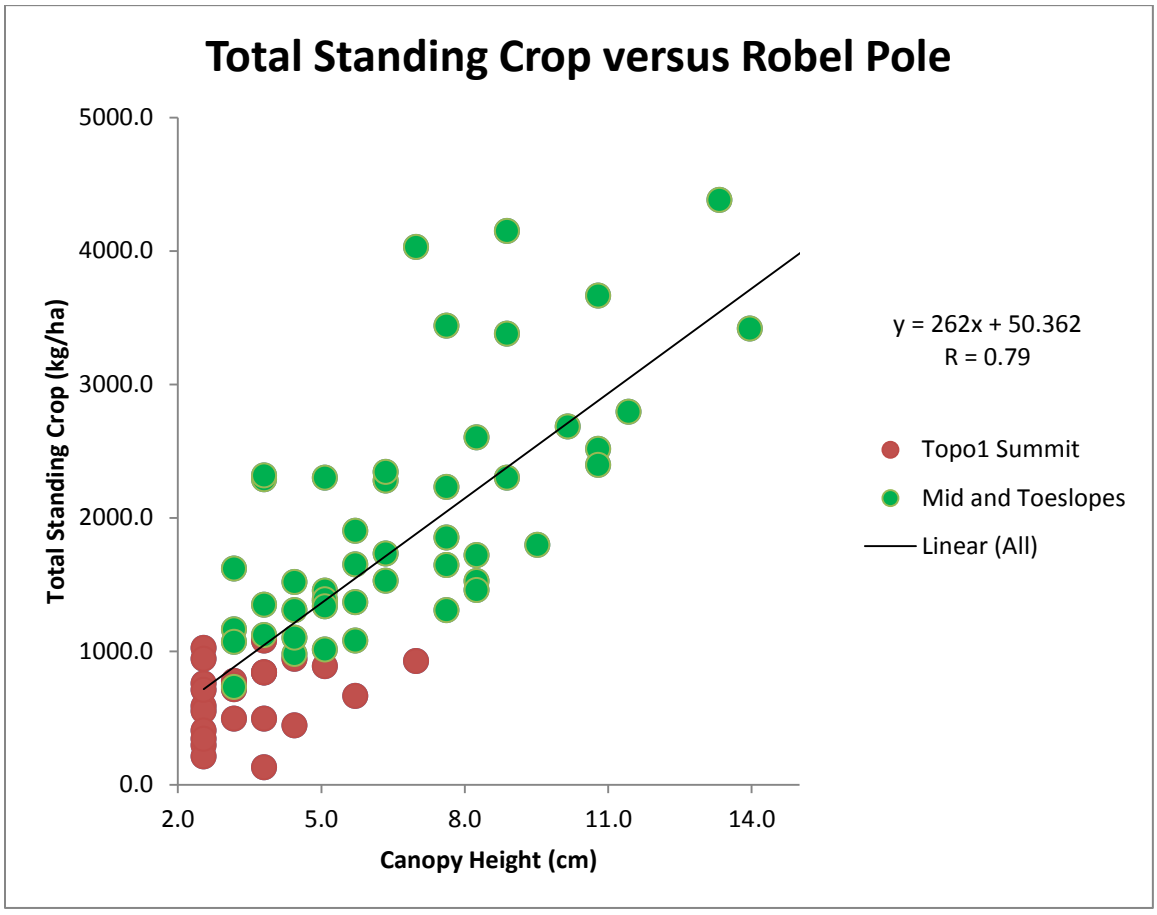

Figure 6. Total standing crop (TSC) versus Robel pole measurements collected at 72 field sites.

Application of both SWIR-SR (ρ_{2215} / ρ_{1650}; Fig. 7) and SWIR Difference Vegetation Index (SWIRDVI; (ρ_{1650} - ρ_{2215}) / (ρ_{1650} + ρ_{2215})) resulted with the same correlation coefficients (R = -0.66) in all 72 points. For this reason there will not be a chart demonstrating this correlation for SWIRDVI; (ρ_{1650} - ρ_{2215}) / (ρ_{1650} + ρ_{2215}). Figure 7 demonstrates a good summit cluster and as SWIR-SR (ρ_{2215} / ρ_{1650}) values decreases TSC (kg/ha) increases.

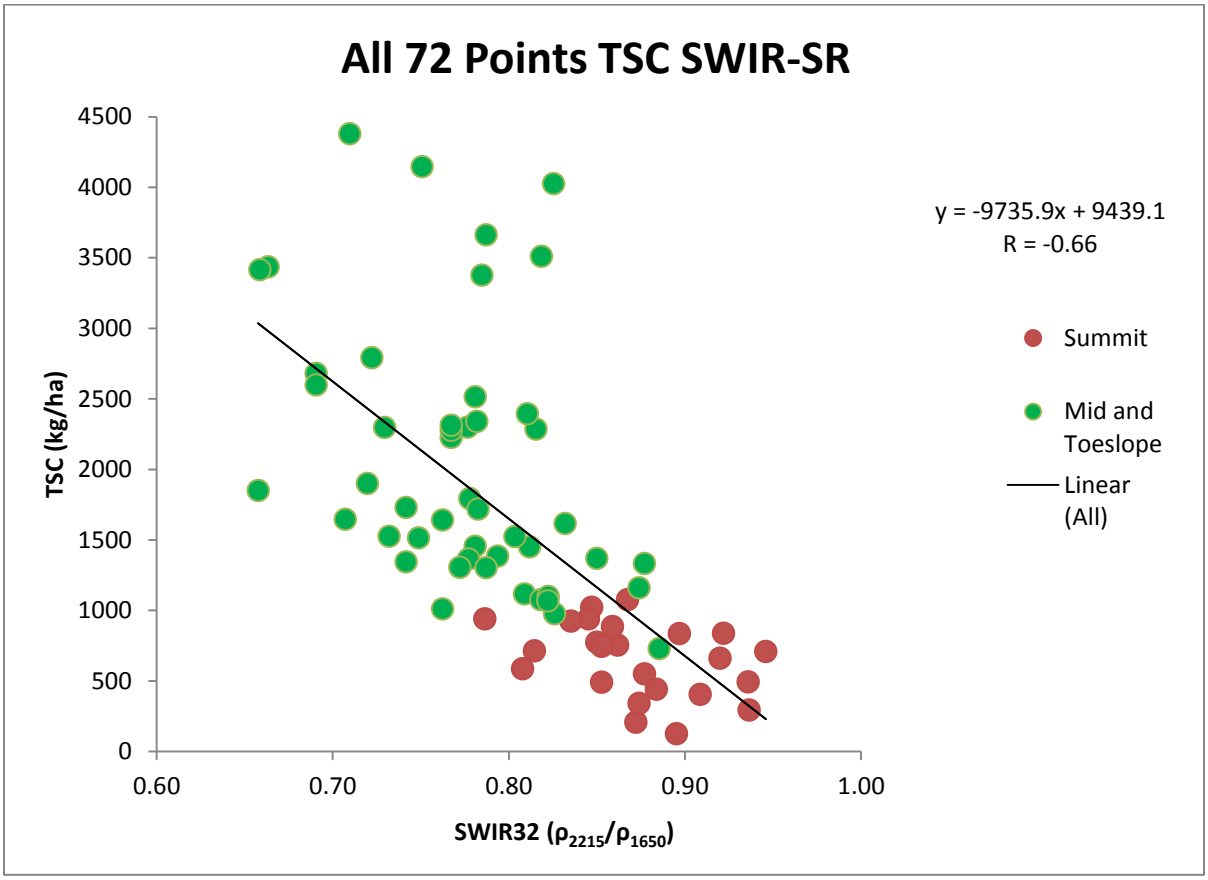

Figure 7. Chart of TSC and SWIR-SR (ρ_{2215}/ρ_{1650}) for all 72 points.

Non-Photosynthetic Vegetation (NPV)

In Figure 8 (NPV versus Robel pole) the NPV relationship to topographic position is very similar to TSC versus Robel pole (Fig. 6) the dissimilarity is in the correlation coefficients for NPV where R = 0.81 and TSC R = 0.79. The non-photosynthetic vegetation clippings for 72 sites yielded estimates ranging from 127 to 4322 kg ha $^{-1}$ with a mean of 1453 kg ha $^{-1}$.

As seen in TSC (Fig.7) there is a good linear negative correlation and a good summit data cluster. The correlation coefficient for NPV in the 72 sites (Fig. 9) with R = -0.60. The relationship for NPV is similar to the relationship seen for TSC and is to be expected because the canopy at this time of the year is mostly comprised of NPV.

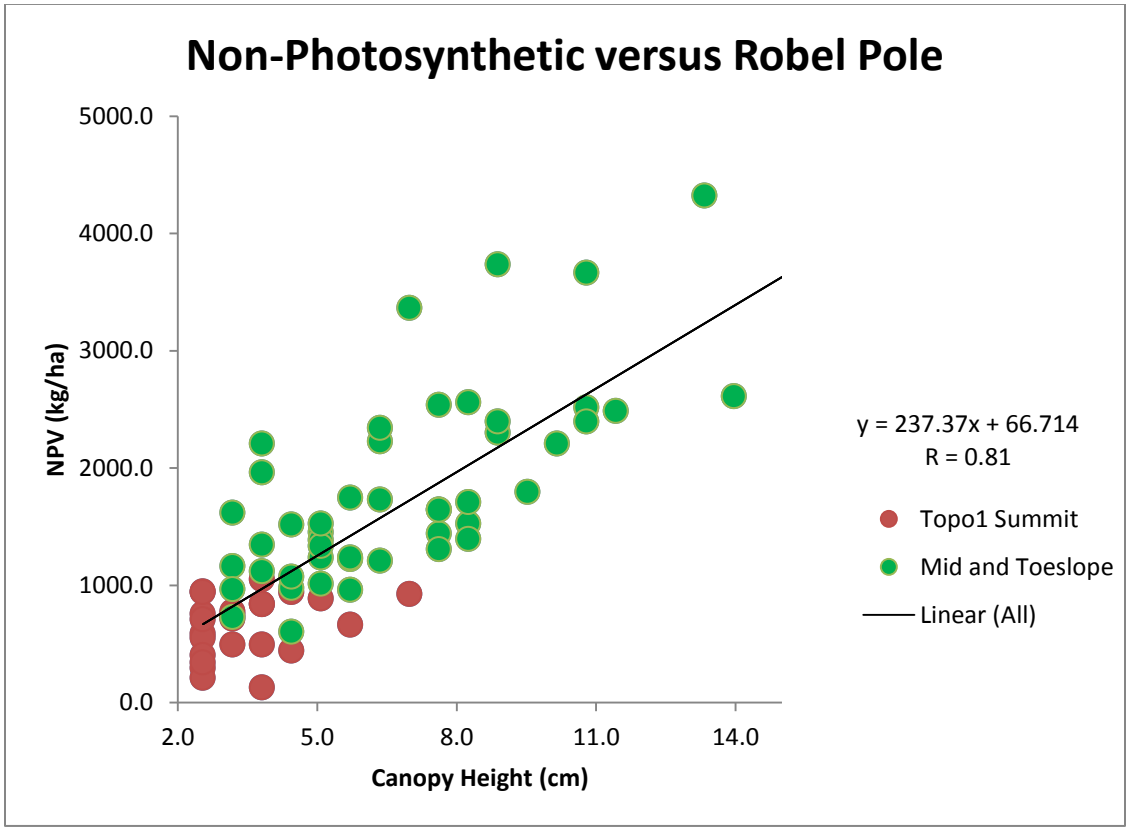

Figure 8. Chart of non-photosynthetic vegetation (NPV) versus Robel pole measurements.

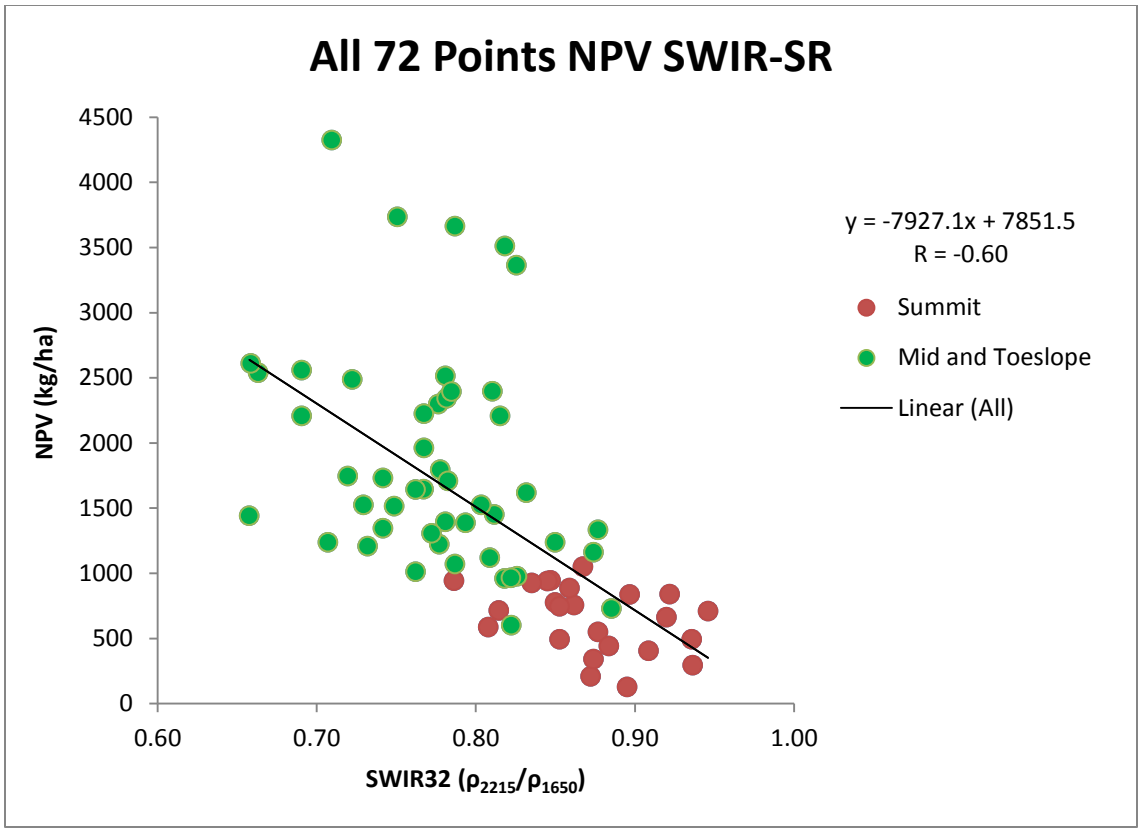

Figure 9. Chart of NPV and SWIR-SR (ρ_{2215}/ρ_{1650}) for the 72 points.

Bare Ground Percent (%BG)

The ocular measurements for the percent bare ground varied from 0% to 58% with a mean of 16%. The SWIR-SR (ρ_{2215}/ρ_{1650}) has a positive linear correlation and a correlation coefficient R = 0.69 for the 72 field points (Fig. 10). The summits are not clustered together as they were for both TSC and NPV. The summits have a good linear correlation with an R = 0.64 whereas the mid- and toeslopes have an R value of 0.46 indicating only a fair correlation. Based on these differences in R values the summit data was plotted separately from the mid- and toeslope combined data with results presented in Figures 11 and 12.

The spectral index SWIRDVI (($\rho_{1650} - \rho_{2215}$) / ($\rho_{1650} + \rho_{2215}$); Fig. 13) has a similar correlation coefficient for %BG at all 72 sites as SWIR3-SR (ρ_{2215}/ρ_{1650}) with an R = 0.67.

The summit data points resulted in a R = 0.64 (Fig.14) and for the mid and toeslopes R = 0.46 (Fig. 15).

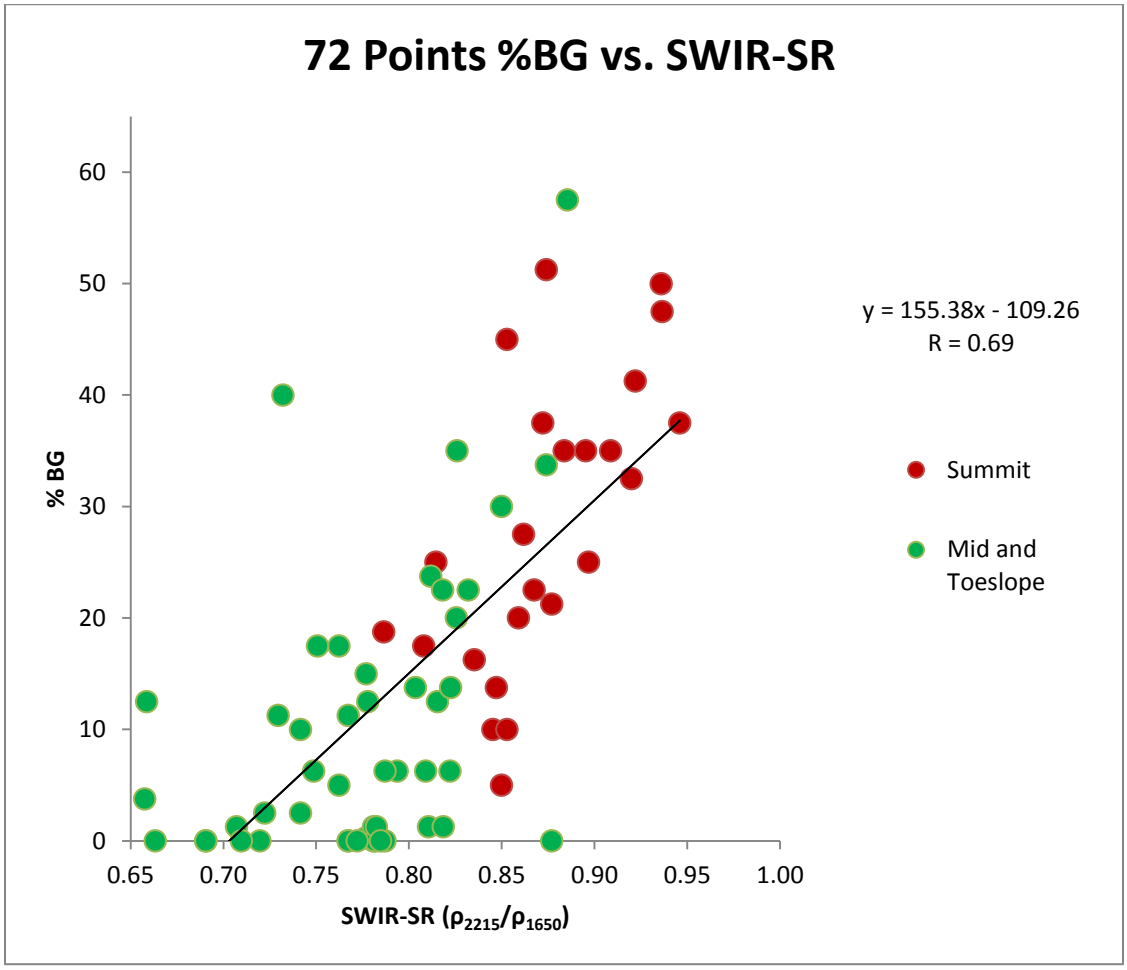

Figure 10. Chart of bare ground percent (%BG) and SWIR-SR (ρ_{2215}/ρ_{1650}) for the 72 points.

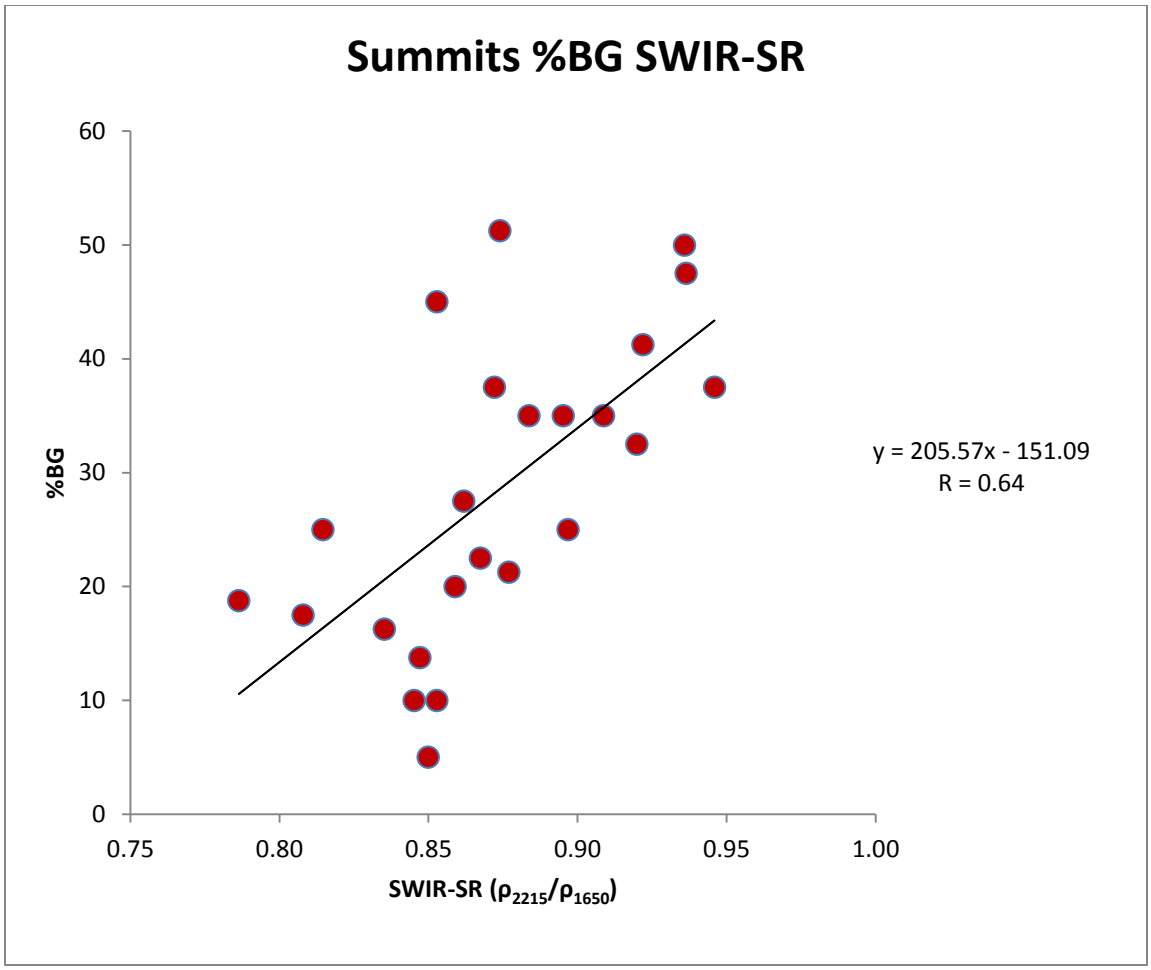

Figure 11. Chart of bare ground percent (%BG) and SWIR32 (ρ_{2215}/ρ_{1650}) for the summits.

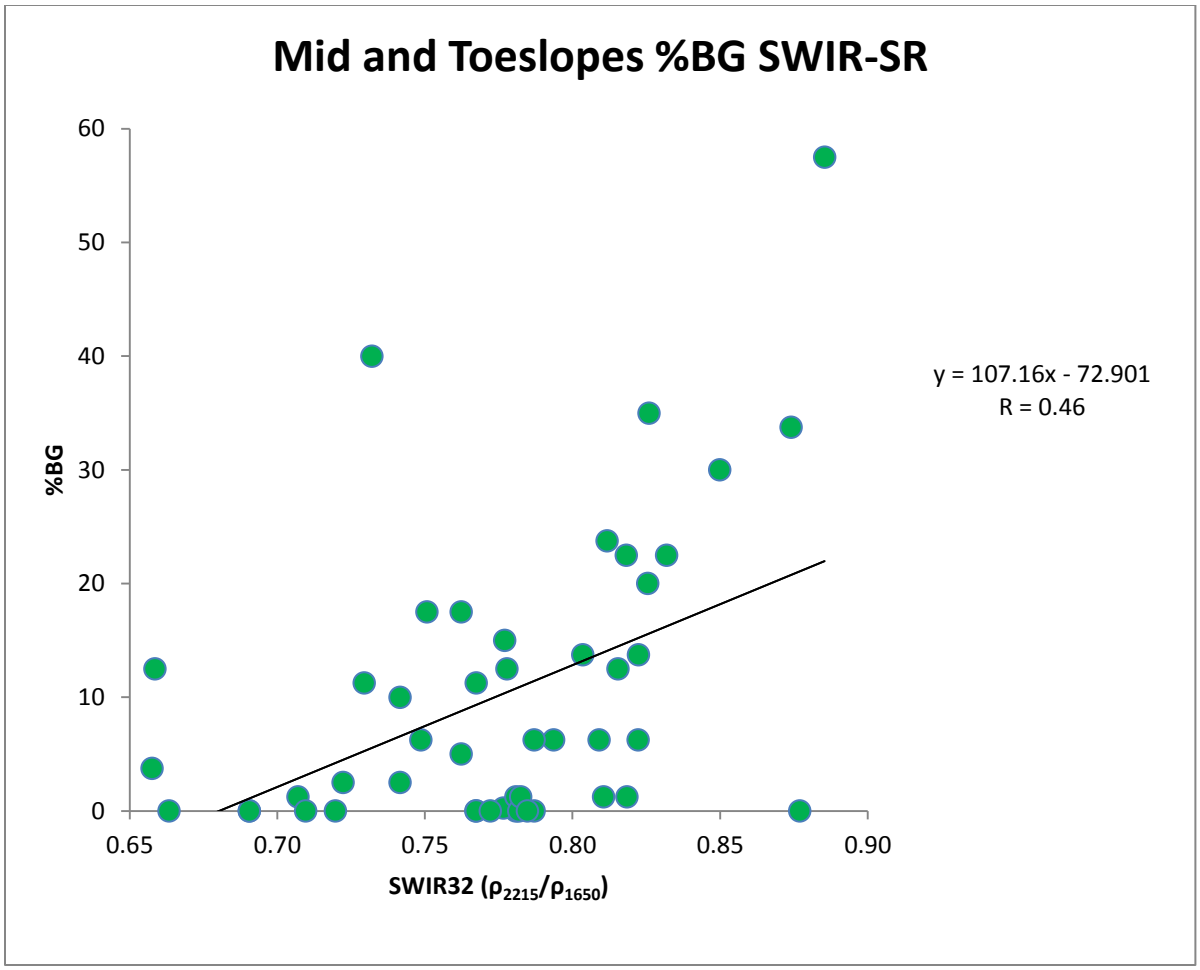

Figure 12. Chart of bare ground percent (%BG) and SWIR-SR (ρ_{2215}/ρ_{1650}) for the mid- and toeslopes.

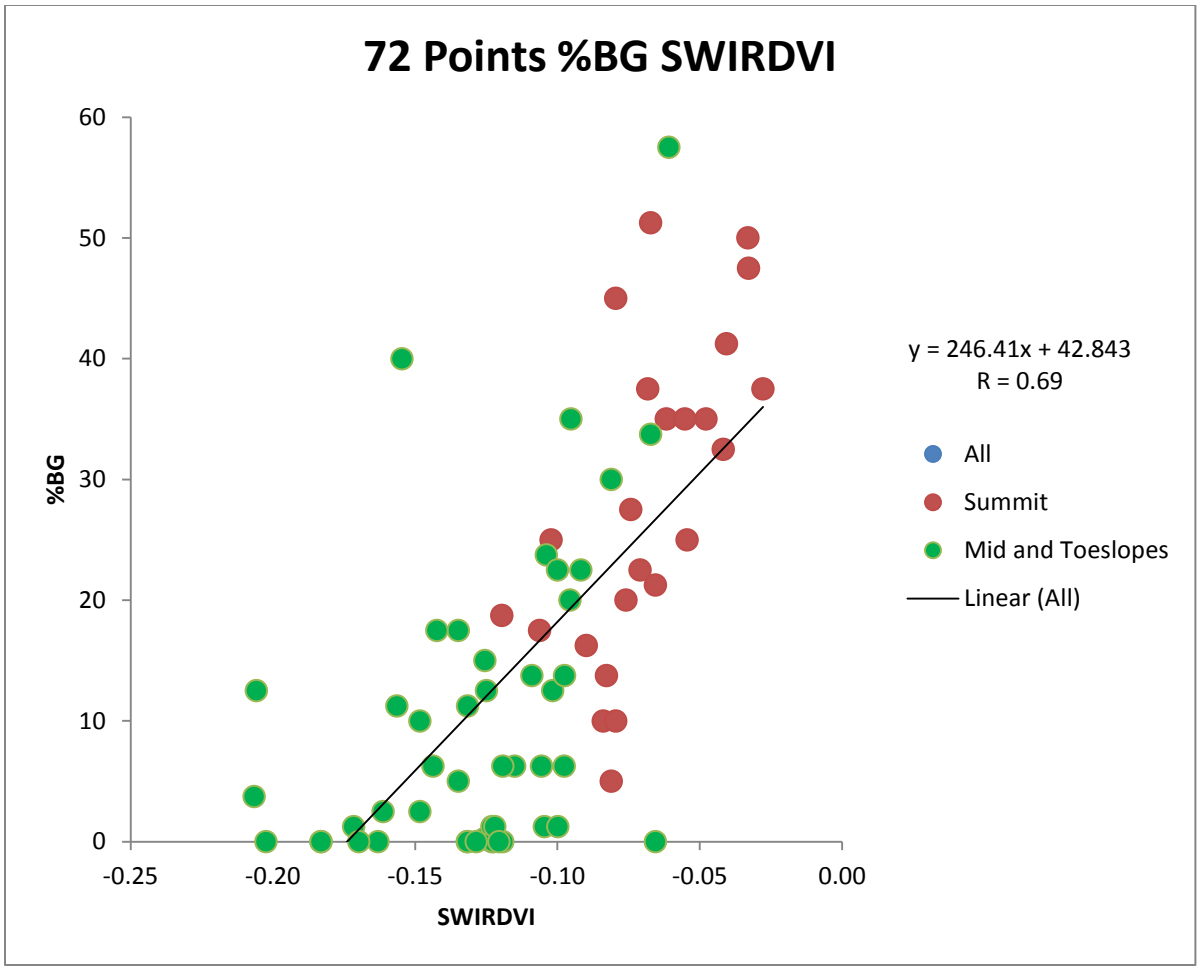

Figure 13. Chart for %BG and SWIRDVI $(\rho_{1650} - \rho_{2215}) / (\rho_{1650} + \rho_{2215})$ for the 72 points.

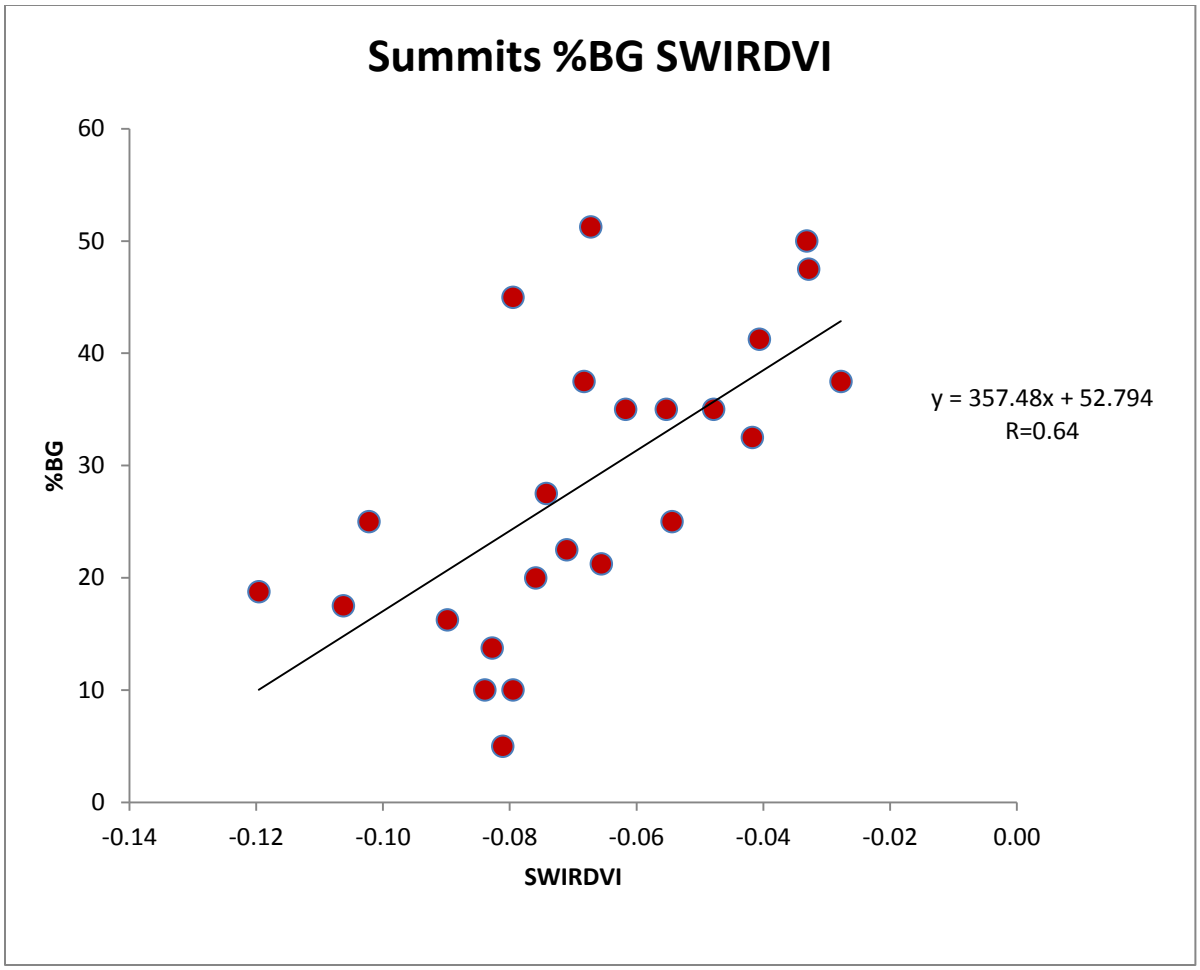

Figure 14. Chart of %BG and SWIRDVI $(\rho_{1650} - \rho_{2215}) / (\rho_{1650} + \rho_{2215})$ for the summits.

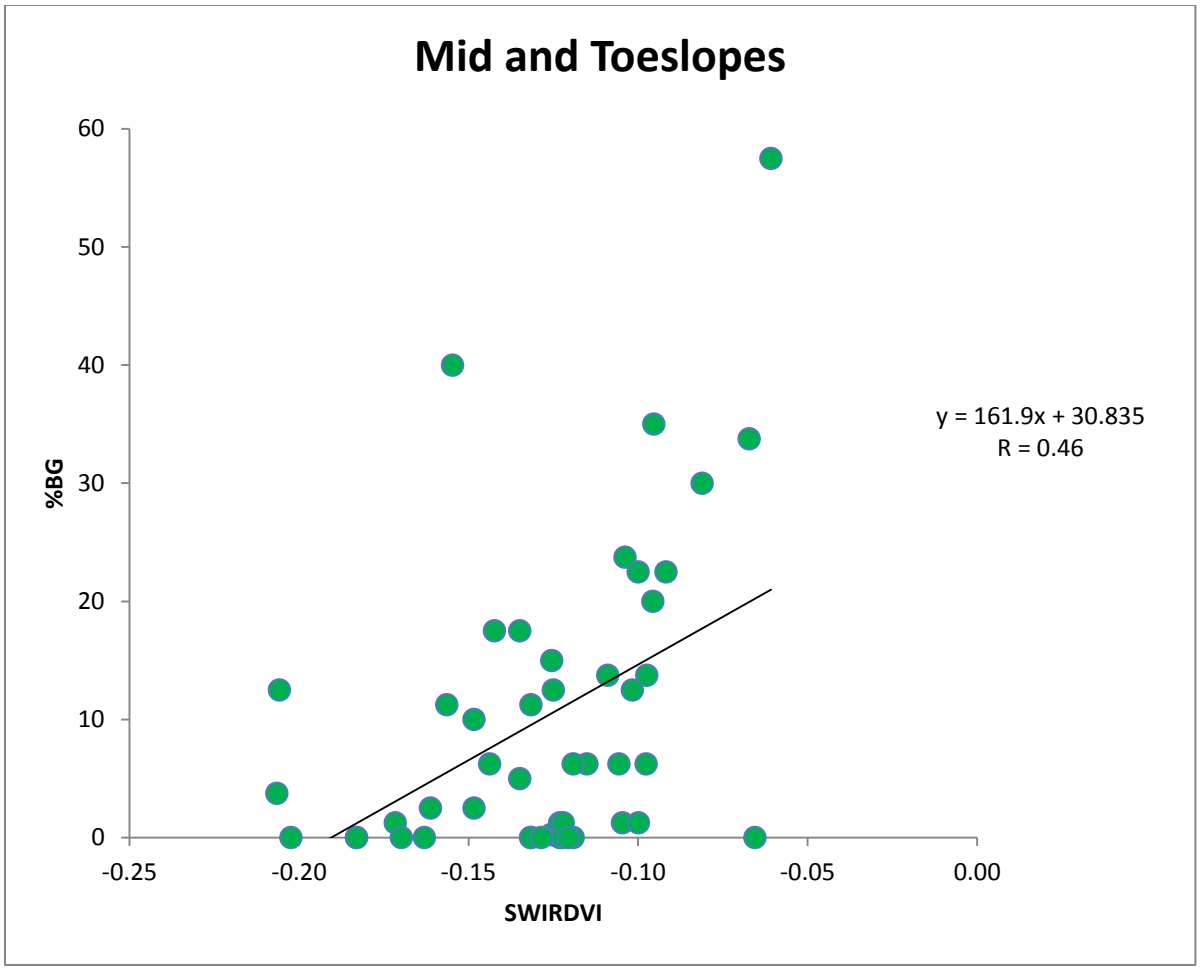

Figure 15. Chart of %BG and SWIRDVI $(\rho_{1650} - \rho_{2215}) / (\rho_{1650} + \rho_{2215})$ for the mid- and toeslopes.

CHAPTER IV

DISCUSSION

This study builds on previous work by Phillips et al. (2012, 2013), but rather than assessing grassland vegetation at the height of the growing season as was done in Phillips et al. (2012), focusing on PV and subsequently analyzing the validity of MODIS and AVIRIS hyperspectral data in Phillips et al. (2013) to create a remote sensing model, this study specifically addresses Landsat TM data applied to late season senescent vegetation. The intent is to develop remote sensing applications for grassland management particularly as it relates to bird habitat and winter forage for wildlife and livestock.

Linear Regression Model Analysis

The Landsat TM linear regression model for all 72 points is good as indicated in Figures 7 and 9 for TSC and NPV versus SWIR-SR (ρ_{2215}/ρ_{1650}). The inverse relationship in Figures 7 and 9 correspond to the effect of increasing above ground biomass producing a lower SWIR32 value.

Phillips et al. (2013) as well as other researchers (e.g., Fitzgerald and Ustin 1992) found a correlation between biomass and AVIRIS reflectance data in the SWIR region. Other researchers (Kokaly et al. 2003; Daughtry et al. 2005) found absorption increased in SWIR with increasing lignin and cellulose content. Phillips et al. (2013) also found that: a) this increased absorption leads to lower values for SWIR-SR ($\rho_{2128/1642}$) as TSC increases, and b) the higher values

indicate less TSC and more bare soil (Guerschman et al. 2009). Similarly, lower values of SWIR3/SWIR2 (ρ_{2215}/ρ_{1650}) were correlated with higher values of TSC and NPV and less bare soil.

General Linear Model

When the SWIR spectra are used alone it is challenging to delineate both %BG and TSC because these materials have similar reflective characteristics. Consequently, some researchers have used NDVI combined with VIs in the SWIR region to assist in separating and estimating %BG and TSC. Here, the %BG model was most predictive if SWIR32, ND71 and % water were included in the model

Total Standing Crop

The summit data points plot with significantly higher values of SWIR3-SR (ρ_{2215}/ρ_{1650}) in Figure 7, whereas the mid and toeslope values fall at the lower end of SWIR3-SR (ρ_{2215}/ρ_{1650}).

Summit data points are tightly clustered with a range of SWIR values from 0.79 to 0.94 and TSC range from 127 to 1077 kg/ha. This is compared to corresponding ranges for the mid and toeslope combined data, which range from 0.66-0.89 for SWIR values and 729 to 4380 kg/ha for above ground biomass. These significantly different value ranges corresponding to different topographic locations suggest that these two data subsets should be treated separately in the model analysis. Again, this is probably related to the observed difference in vegetation type, vegetation height, and percent bare ground.

The significant influence of elevation position on TSC volume has implications for grassland managers and future spectral analyses.

Non-Photosynthetic Vegetation

The correlation coefficient for NPV versus the Robel pole measurement R = 0.81 (Fig. 8) and is similar to that seen in the TSC R = 0.79 (Fig. 6), which is to be expected based on the direct strong correlation between TSC and NPV.

Bare Ground Percent

The mid and toeslope cross plot has a low R = 0.46 (Fig. 12) and the data were explored further. The %BG midslope (Fig. 16) R = 0.62 whereas the %BG toeslope (Fig. 17) R = -0.004.

The poor correlation between the toeslope data ocular readings and the SWIR data taken from Landsat 30 m (900 m^2) resolution imagery indicates that Landsat data cannot accurately estimate r %BG for the toeslope positions.

From the summit and midslope positions, correlations between Landsat data-based estimates and %BG are stronger, with R = 0.64 and R = 0.62, respectively. This suggests that Landsat TM data correlates well with 0.187-m^2 Daubenmire frame ocular estimates of %BG for summit and midslope elevations.

The plot of summit and midslope excluding toeslope yields a correlation coefficient R = 0.73 (Fig. 18) indicating that %BG estimates derived from SWIR32 (ρ_{2215}/ρ_{1650}) Landsat TM VI has some validity when applied at the proper scale (LOI = 60,000+ ha) but not at the single pixel scale (30 m^2).

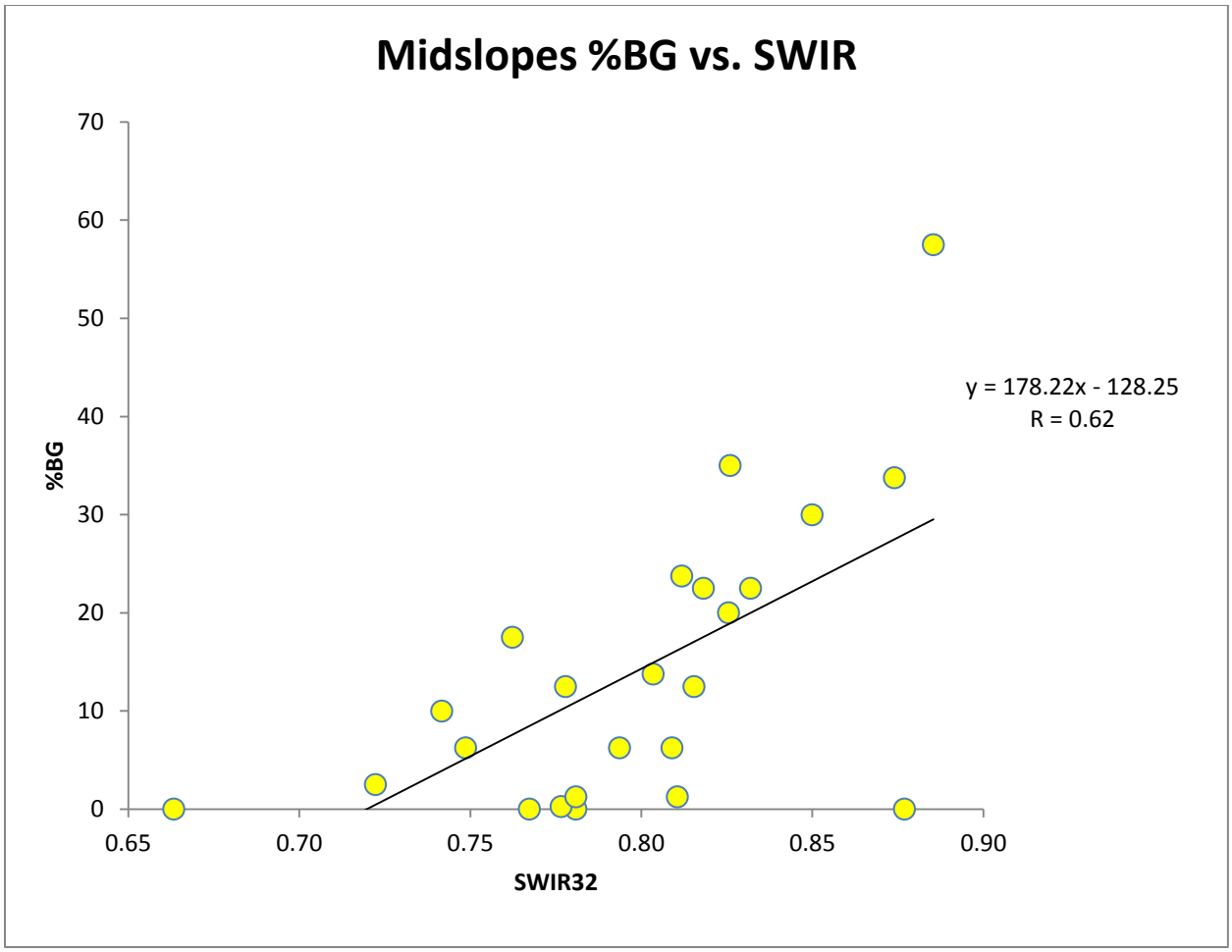

Figure 16. Chart of %BG and SWIR-SR (ρ_{2215}/ρ_{1650}) for the midslopes.

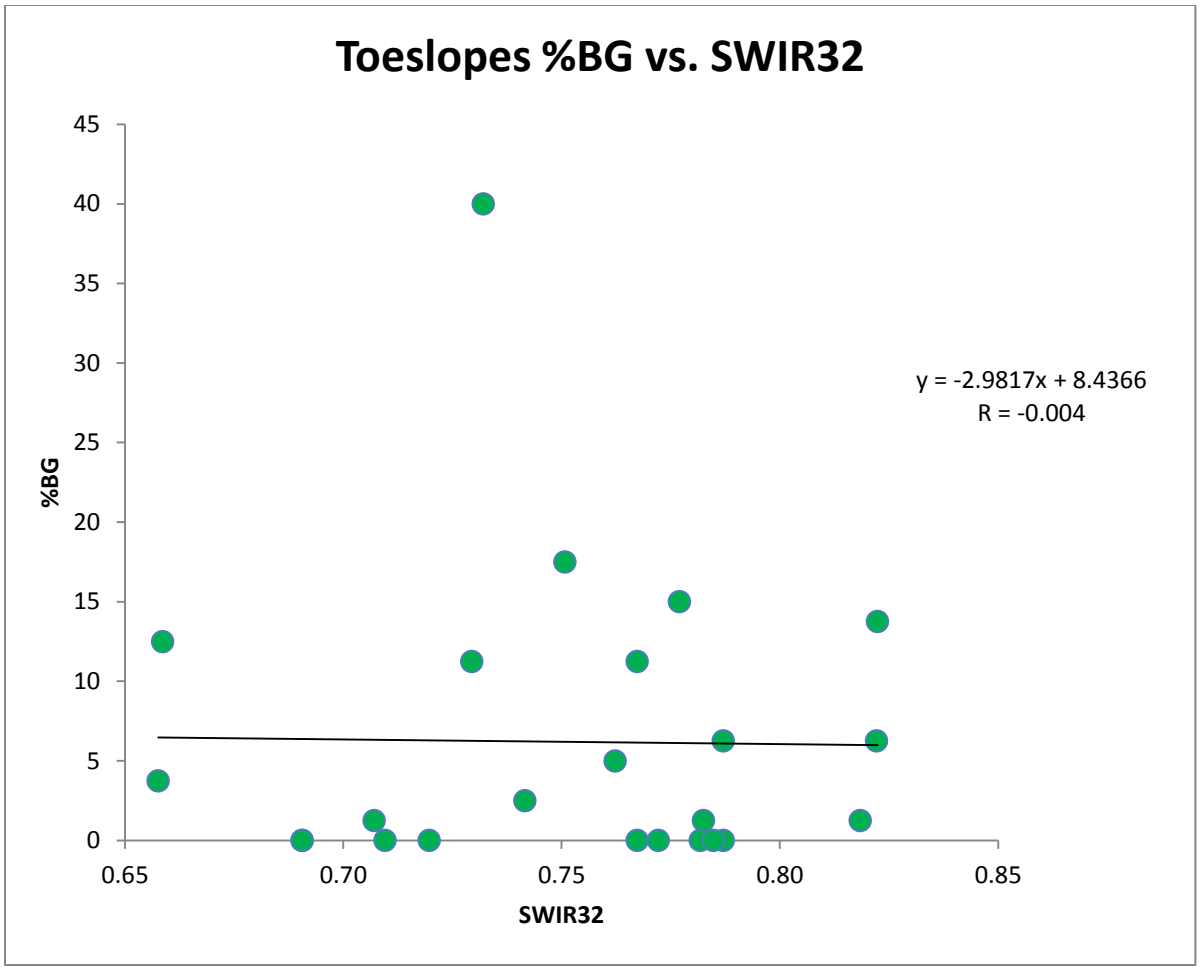

Figure 17. Chart of %BG and SWIR-SR (ρ_{2215}/ρ_{1650}) for the toeslopes.

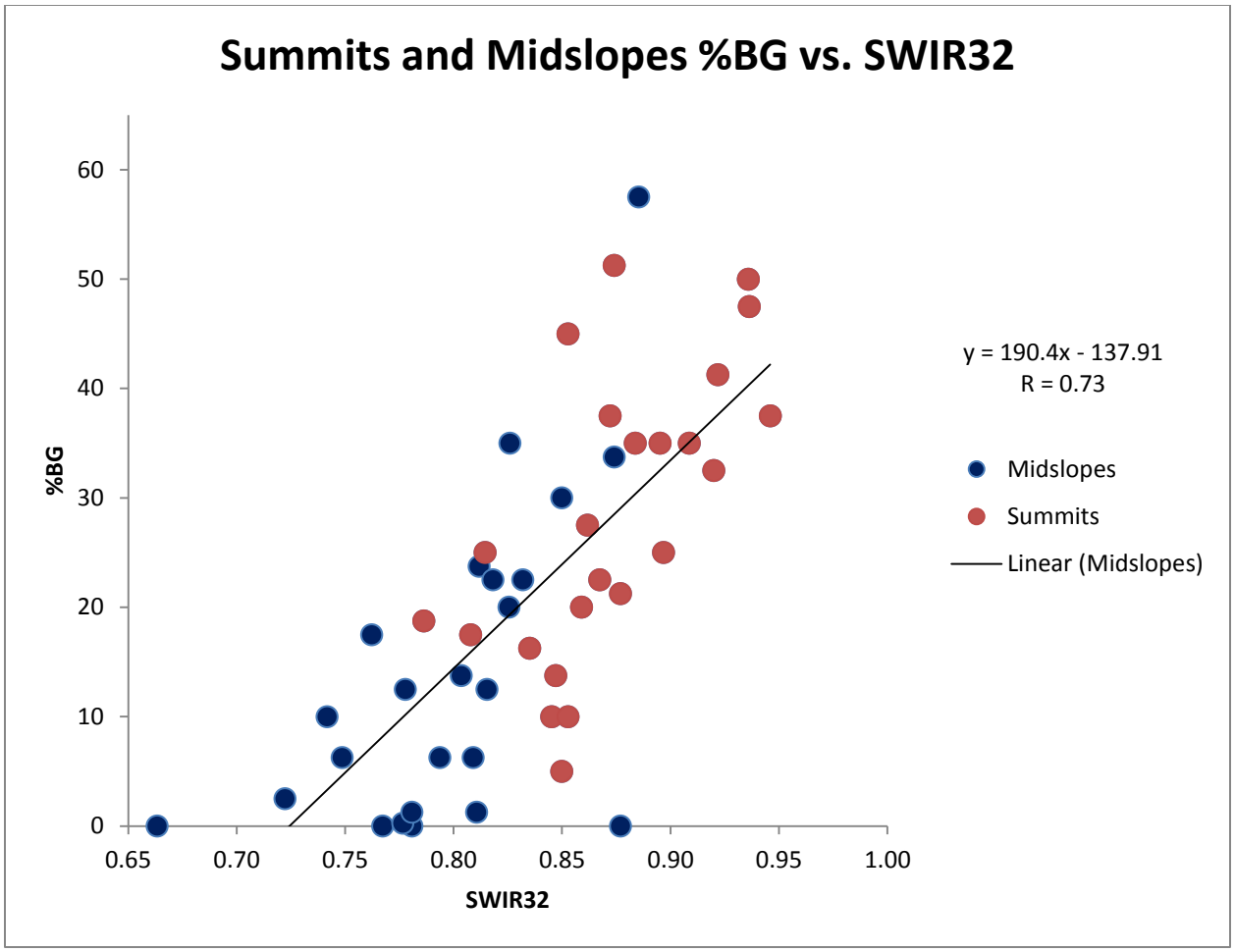

Figure 18. Chart of %BG and SWIR-SR (ρ_{2215}/ρ_{1650}) for both summits and midslopes.

Significant variability in %BG over short distances is dramatically illustrated in Figure 19. This graphic illustration is not atypical of the study site. This high variability at lower resolutions than the Landsat TM pixel scale may be the primary cause of the low correlation between %BG and Landsat TM imagery, especially at toeslope elevations.

Figure 19. Grand River National Grassland bare ground. (Photo courtesy of Dr. Rebecca Phillips)

Canopy Structural Variables and Spectral Response Relationships

As in the previous graphs (Figs. 6 and 8), Robel pole (canopy height (cm)) versus SWIR - SR (ρ_{2215} / ρ_{1650}; Fig. 20) comparison clearly demonstrates topographic position correlation, as illustrated by the color clustering. The canopy height (Robel pole data) decreases as SWIR-SR value increases (inverse relationship; i.e. summit values cluster at shorter canopy height whereas mid and toeslope values indicate taller canopy).

Comparison of R values for TSC and NPV versus Robel pole yield R = 0.79 and 0.81, respectively, whereas SWIR-SR versus Robel pole (Canopy Height) has an R of 0.58. From this it appears that although the correlation coefficient derived from satellite imagery is somewhat less than that derived from field data, it is still valid. Landsat TM imagery obtainable at little or no cost every 8 days if desired, with blanket coverage over an area of interest provides a workable alternative or complement to labor intensive field data collection involving limited data points and human induced measurement variations.

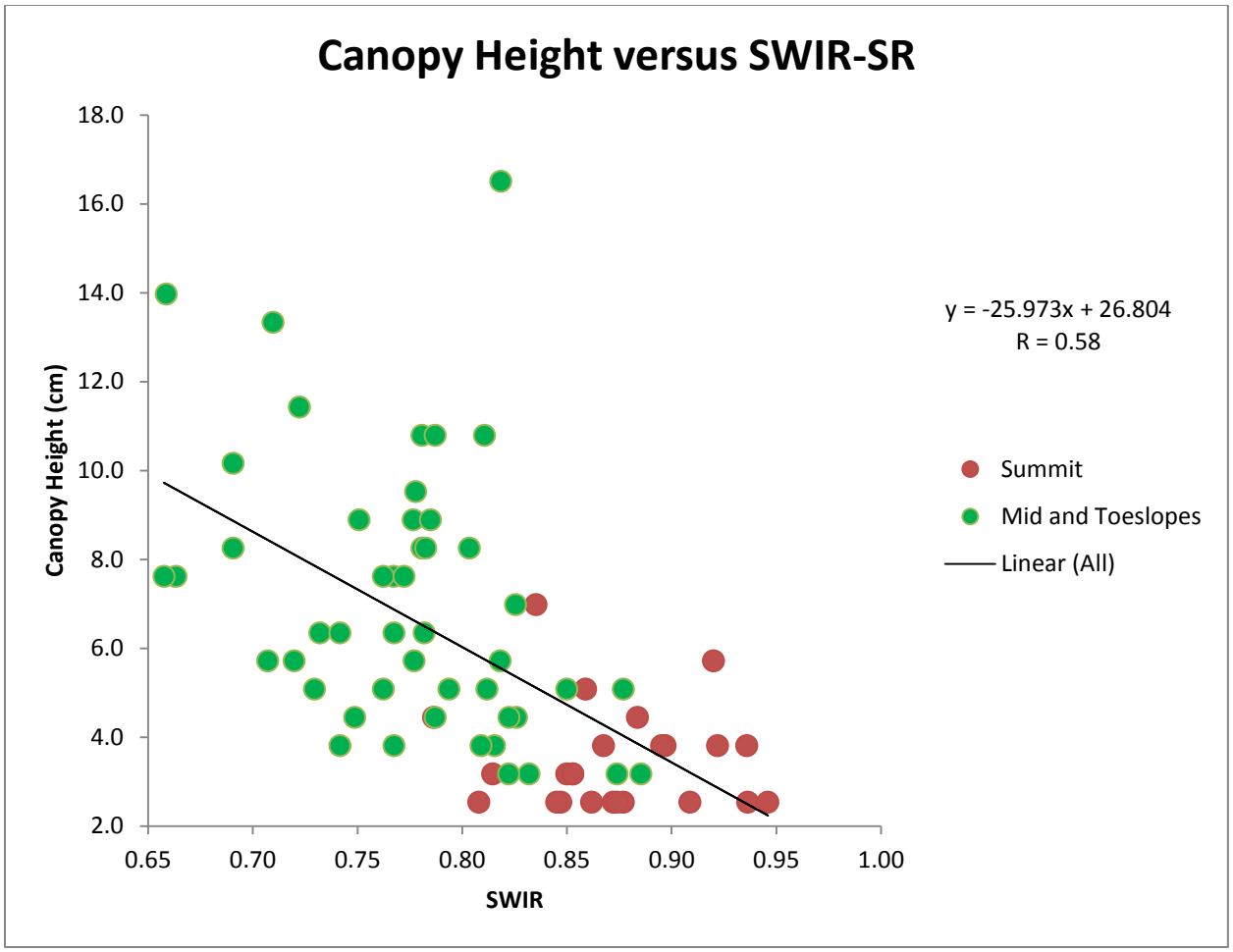

Figure 20. Canopy height measured using the Robel pole versus SWIR-SR index collected at 72 field sites.

Mapping Modeled Canopy Attributes

Comparison of predictive model R values from Table 3 (Phillips et al. 2013) showing -0.87, -0.82, and 1 for TSC, NPV and %BG, respectively, compared to Table 4 (this study) with R values -0.66, -0.60, and 0.69 for TSC, NPV and %BG, respectively, using Landsat TM data were comparable except for %BG. This supports the validity of the application of moderate resolution multispectral remote sensing imagery to the assessment of grassland attributes relative to avian habitat preservation and livestock and wildlife winter feed conditions.

For example, the Low HRI in Figure 3, is shown in Figure 21 with %BG derived from SWIR data analysis in this study. Results are comparable to those seen in Figure 27. The aqua colored rectangular area in the northeast corner of Figure 21 with %BG range of 30-40% is a plowed field and is also seen in Figure 27 (royal blue) representing <127 kg/ha TSC. The lime green swath trending diagonally from northwest to southeast in Figure 21 is comparable to the yellow areas in Figure 27. This good correlation of %BG mapping using SWIR from this study to the predictive model TSC values mapped in Figure 27 support the validity of using Landsat TM data for assessing grassland vegetation parameters.

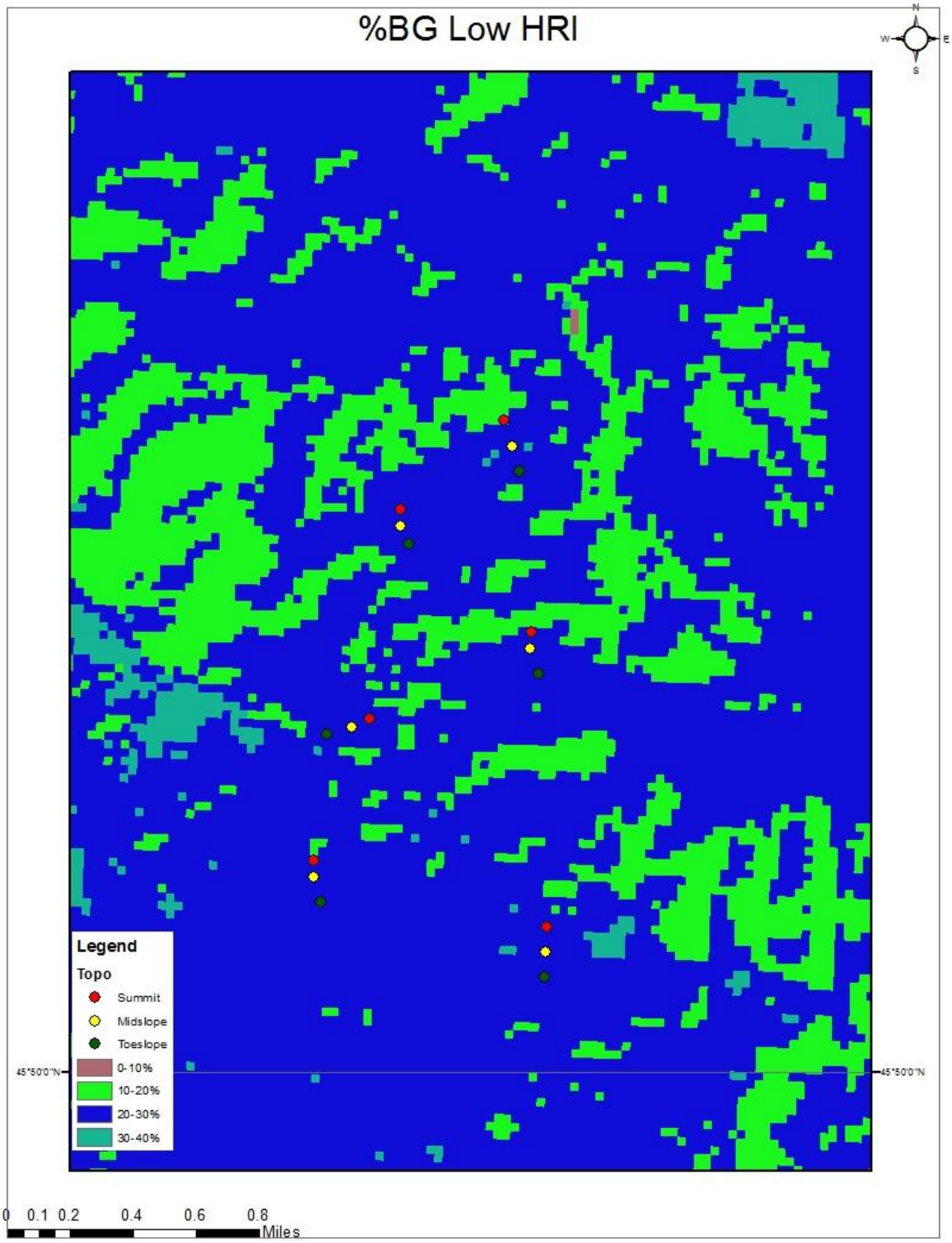

Figure 21. Map of six field sites using bare ground percent estimates in Low HRI.

.

Table 3. Predictive model R and predictive spectral index R for variables TSC and NPV and %BG. Each variable uses all data (Phillips et al. 2013).

Predictive Canopy Attributes	**Predictive Spectral Index R**	**Vegetation Index (VI)**
TSC (total biomass)	-0.87	SWIR-SR (ρ_{2215}/ρ_{1650})
NPV (brown vegetation)	-0.82	SWIR-SR(ρ_{2215}/ρ_{1650})
%BG (percent bare ground)	1	SWIR-SR (ρ_{2215}/ρ_{1650}) and ND71

Table 4. Correlation coefficient R for variables TSC and NPV and %BG. Each variable uses all data (Phillips et al. 2013).

Canopy Attributes	R	Vegetation Index (VI)
TSC (total biomass)	-0.66	SWIR-SR (ρ_{2215}/ρ_{1650})
NPV (brown vegetation)	-0.60	SWIR-SR (ρ_{2215}/ρ_{1650})
%BG (percent bare ground)	0.69	SWIR-SR (ρ_{2215}/ρ_{1650})

The Grand River National Grassland Landsat TM imagery (Fig. 22) is the study area with the 72 field sites. Figures 22-29 depict TSC (kg ha -1) from Landsat TM imagery.

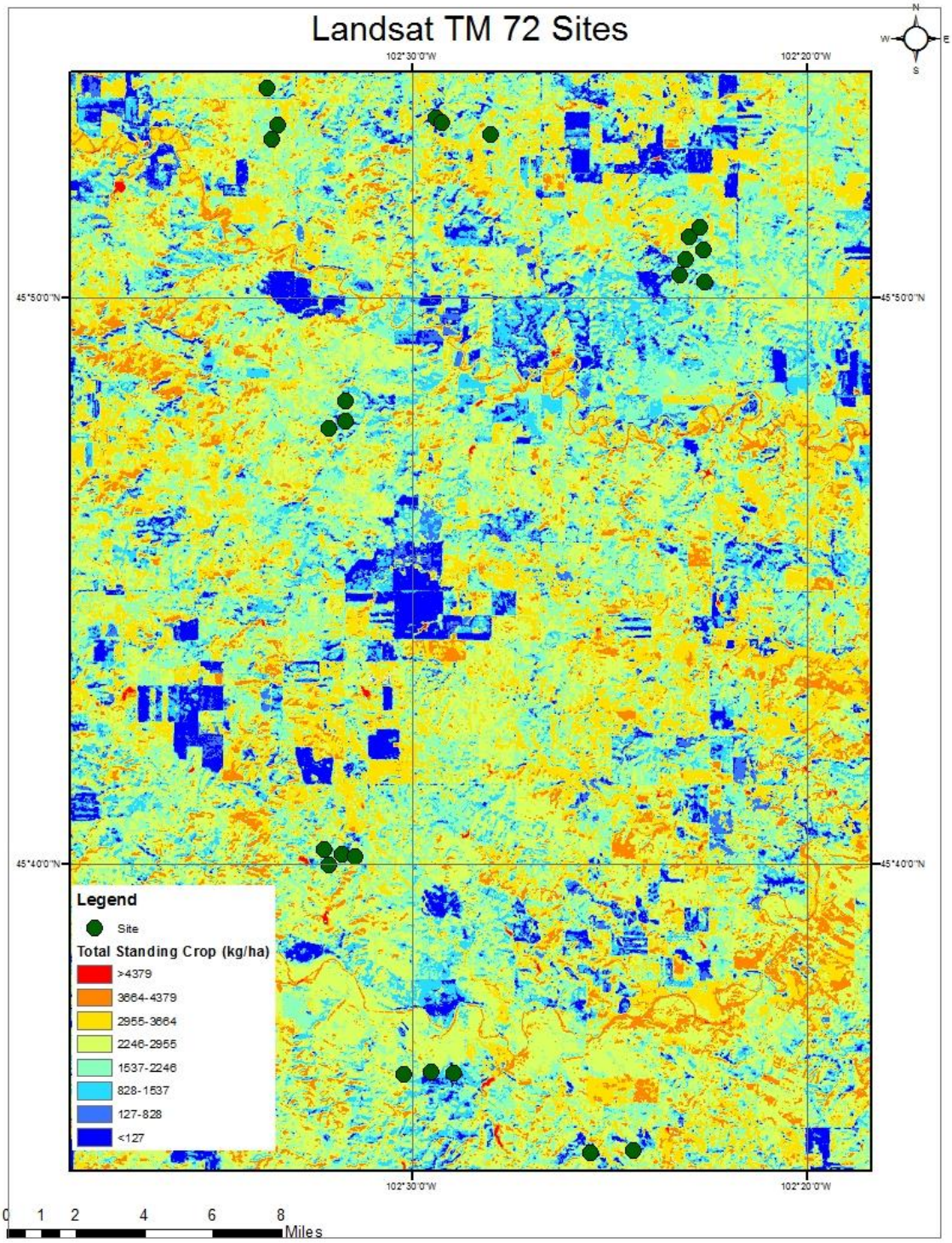

Figure 22. State of South Dakota. Grand River National Grassland Landsat imagery with the 72 study sites.

CHAPTER V

CONCLUSION

Results of this study are comparable to those in previous work (Phillips et al. 2012, 2013) Application of Landsat TM moderate resolution multispectral data can be used to augment currently employed field techniques such as Robel pole and clippings to assess TSC, NPV, and %BG conditions for management of Northern Great Plains Grasslands.

Statistical analyses from this study indicate good results may be obtained for TSC and NPV using SWIR-SR collected at the Landsat sensor. However, attempting to use Landsat data to estimate %BG, particularly in the toeslope topographic position must be applied with caution, as evidenced by R value near 0 (Fig. 17)

If %BG is needed, remote sensing imagery with a small footprint should be used; perhaps IKONOS or Quick Bird would produce more valid results as well as utilizing NDVI to monitor %BG (Baghzouz et al. 2010). The vegetation indices in the SWIR region developed from hyperspectral imagery (i.e. AVIRIS in Phillips et al. 2013) can also be used with Landsat TM imagery. Hyperspectral imagery can be very expensive whereas Landsat is free and easier to access. This can provide a basis for complementing and refining grassland management practices.

This ongoing research in the Northern Great Plains Grasslands has a potential to stimulate future research into the application of remote sensing to identify and map the vertical

structure of vegetation and above biomass specific to bird species preferred habitat and/or nesting “hotspots” as well as assessment of post growing season livestock feed conditions.

This research was conducted in the Northern Great Plains region with mixed grasses being dominant. If applied elsewhere (i.e. arid southwestern U.S. and tallgrass prairie, etc.) it would need to be calibrated to local ecosystem field data as was done in this study

REFERENCES

Asner, G. P., 1998, "Biophysical and Biochemical Sources of Variability in Canopy Reflectance." *Remote Sensing of Environment*, 64: 234– 253.

Baghzouz, M., Devitt, D. A., Fenstermaker, L. F., and M. H. Young, 2010, "Monitoring Vegetation Phenological Cycles in Two Different Semi-Arid Environmental Setting Using a Ground-Based NDVI System: A Potential Approach to Improve Satellite Data Interpretation." *Remote Sensing*, 2: 990-1013; doi:10.3390/rs2040990.

Bakker, K. K., Naugle, D. E. and K. F. Higgins, 2002, "Incorporating Landscape Attributes into Models for Migratory Grassland Bird Conservation." *Conservation Biology*, 16:1638-1646.

Benz, U. C., Hofman, P., Willhauck, G., Lingenfelder, I., and M. Heynen, 2004, "Multi-Resolution, Object-Oriented Fuzzy Analysis of Remote Sensing Data for GIS-Ready Information." *ISPRS Journal of Photogrammentry & Remote Sensing*, 58(3-4):239-258.

Bittencourt, H. R. and R. T. Clarke, 2003, "Logistic Discrimination Between Classes with Nearly Equal Spectral Response in High Dimensionality." Pages 3784-3750 in IEEE International Geoscience and Remote Sensing Symposium, Toulouse, France.

Block W. M. and K. A. Morrison, 1987, "On Measuring Bird Habitat: Influence of Observer Variability and Sample Size." *Condor,* 89:241-251.

Curran, P. J., 1983, "Multispectral Remote Sensing for the Estimation of Green Leaf Area Index." *Philosophical Transactions of the Royal Society of London, Series A: Mathematical, Physical, and Engineering Sciences,* 309:257– 270.

Daubenmire, R., 1959, "A Canopy-Coverage Method of Vegetational Analysis." *Northwest Science,* 33:43-64.

Daughtry, C. S. T., Hunt, E. R. J., Doraiswamy, P. C., and J. E. McMurtrey III, 2005, "Remote Sensing the Spatial Distribution of Crop Residues." *Agronomy Journal*, 97:864-871.

Dauwalter, D. C., W. L. Fisher, and K. C. Belt, 2006, "Mapping Stream Habitats with a Global Positioning System: Accuracy, Precision, and Comparison With Traditional Methods." *Environmental Management,* 37:271-280.

Elvidge, C. D., and Lyon, R.J.P. 1985, "Influence of Rock-Soil Variation on the Assessment of Green Biomass." *Remote Sensing of Environment,* 17:265-279.

Feldesman, M. R. 2002, "Classification Trees as an Alternative to Linear Discriminant Analysis." *American Journal of Physical Anthropology,* 119:257-275.

Fitzgerald, M. and S. L. Ustin, 1992, "Measuring Dry Plant Residues in Grasslands: A Case Study Using AVIRIS." *Pasadena, CA: Summaries of the Third Annual JPL Airborne Geoscience Workshop*, 3 pages.

Guerschman, J. P., Hill, M. J., Renzullo, L. J., Barrett, D. J., Marks, A. S., and E. J. Botha, 2009, "Estimating Fractional Cover of Photosynthetic Vegetation, Non-Photosynthetic Vegetation and Bare Soil in the Australian Tropical Savanna Region Upscaling the EO-1 Hyperion and MODIS Sensors." *Remote Sensing of Environment*, 113:928-945.

Hansen, K., 2008, "Plants of the Grand River and Cedar River National Grasslands: 2008." *USDA-Forest Service, Dakota Prairie Grassland, internal report,* Washington, DC p.56.

Herkert, J. R., 1995, "An Analysis of Midwestern Breeding Bird Population Trends; 1966-1993." *American Midland Naturalist,* 135:41-50.

Huete, A.R., Jackson, R.D., and D.F. Post, 1985, "Spectral Response of a Plant Canopy with Different Soil Backgrounds." *Remote Sensing of Environment,* 17:37-53.

Huete, A. R., 1988, "A Soil-Adjusted Vegetation Index (SAVI)." *Remote Sensing of Environment,* 25:295-309.

Huete, A.R., and C. Tucker, 1991, "Investigation of Soil Influences in AVHRR Red and Near-Infrared Vegetation Index Imagery." *International Journal of Remote Sensing,* 12:1223-1242.

Huete, A. R., Liu, H. Q., Batchily, K., and Leeuwen van, W., 1997, "A Comparison of Vegetation Indices over a Global Set of TM Images for EOS-MODIS." *Remote Sensing of Environment*, 59: 440−451.

Irving, B. D., Ruthledge P. L., Bailey A. W., Neath M. A., and D. S. Chanasyk, 1995, "Grass Utilization and Grazing Distribution within Intensively Managed Fields in Central Alberta." *Journal of Range Management*, 48:358-361.

Kershaw, K. A., 1973, "Quantitative and Dynamic Plant Ecology." *American Elsevier Publication Co.*, Inc. 2nd ed. New York, pp. 1-308.

Kokaly, R. F., Despain, D. G., Clark, R. N., and K. E. Livo, 2003, "Mapping Vegetation in Yellowstone National Park Using Spectral Feature Analysis of AVIRIS Data." *Remote Sensing of Environment,* 84:437-456.

Larivière, S. 2003, "Edge Effects, Predator Movements and the Travel-Lane Paradox." *Wildlife Society Bulletin,* 31:315-320.

Limb, R. F., Hickman, K.R., Engle, D.M., Norland, J.E., and S.D. Fuhlendorf, 2007, "Digital Photgraphy: Reduced Investigator Variation in Visual Obstruction Measurements for Southern Tallgrass Prairie." *Rangeland Ecology Management,* 60:548-552.

Marsett, R. C., Qi, J., Heilman, P., Biedenbender, S. H., Watson, M. C., Amer, S., and R. Marsett, 2006, "Remote Sensing for Grassland Management in the Arid Southwest." *Rangeland Ecology and Management,* 59:530-540.

McTainsh, G. H., Leys, J., Carter, D., Butler, H., McCord, A. K., Wain, A., and N. J. McKenzie, 2006, "Monitoring Soil Condition Across Australia: Recommendations from the Expert Panels." *Canberra, Australia: National Committee on Soil and Terrain for the National Land and Water Resource Audit,* pp 43-56.

Milchunas, D. G., Laenroth, W. K., Chapman, P. L., Kazempour, M. K., 1989, "Effects of Grazing, Topography, and Precipitation on the Structure of a Semiarid Grassland." *Vegetation,* 80: 11-23.

Natural Resources Conservation Services (NRCS) 2001, "Mountain plover." *Fish and Wildlife Habitat Management Leaflet.* No. 22.

Omernik, J., 1987, "Ecoregions of the Conterminous United States." *Annals of the Association of the American Geographers,* 77:118-125.

Phillips, R. L., Ngugi, M., Hendrickson, J., Smith, E., and M. West, 2012, "Mixed-Grass Prairie Canopy Structure and Spectral Reflectance Vary with Topographic Position." *Environmental Management,* 50(5):914-928.

Phillips, R.L., West, M., Saliendra, N., Rundquist, B. and D. Poole, 2013, "Prediction of Senescent Rangeland Canopy Structural Attributes with Airborne Hyperspectral Imagery," *GIScience and Remote Sensing,* DOI: 10.1080/15481603.2013.793469.

R Development Core Team, 2010, "R: A Language and Environment for Statistical Computing," *Foundation for Statistical Computing,* Version 2.11.1.

Robel, R. J., J. N. Briggs, A. D. Dayton, and L. C. Hulbert, 1970, "Relationships Between Visual Obstruction Measurements and Weight of Grassland Vegetation." *Journal of Range Management,* 23:296-297.

Rundquist, B. C. 2002, "The Influence of Canopy Green Vegetation Fraction on Spectral Measurements over Native Tallgrass Prairie." *Remote Sensing of Environment,* 81:129–135.

Samson, F. B., and F. Knopf, 1994, "Prairie Conservation in North America." *BioScience,* 44:418-421.

Schultz, A. M., Gibbens R. P., and L. Debano, 1961, "Artificial Populations for Teaching and Testing Range Techniques." *Journal of Range Management,* 14:236-242.

Sjursen, P. 2009, "Grand River National Grassland Robel Pole Inventory." U.S. Forest Service, Bismarck, North Dakota.

Todd, S.W., and R.M. Hoffer, 1998, "Responses to Spectral Indices to Variations in Vegetation Cover and Soil Background." *Photogrammetric Engineering and Remote Sensing,* 64:915-921.

Tucker, C. J., 1979, "Red and Photographic Infrared Linear Combinations for Monitoring Vegetation." *Remote Sensing of Environment,* 8:127–150.

United States Forest Service (USFS), 2001, "Land and Resource Management Plan for the Dakota Prairie Grasslands Northern Region," p 15.

United States Department of Interior, 2013, "The State of the Birds 2013 Report on Private Lands." *North American Bird Conservation Initiative,* U.S. Committee, Washington, D.C. 48 pages.

Uresk D.W., and Benson T.A., 2007, "Monitoring with a Modified Robel pole on Meadows in the Central Black Hills of South Dakota," *Western North American Naturalist,* 67(1):46–50

van Leeuwen, W. J. D., and A. R. Huete, 1996, "Effects of Standing Litter on the Biophysical Interpretation of Plant Canopies with Spectral Indices." *Remote Sensing of Environment,* 55:123-138

Winter, M., D. H. Johnson, and J. A. Shaffer, 2005, "Variability in Vegetation Effects on Density and Nesting Success of Grassland Birds." *USGS Northern Prairie Wildlife Research Center.* Paper 233.

Zhang, Y., Smith, A. M., and M. J. Hill, 2011, "Estimating Fractional Cover Of Grassland Components From Two Satellite Remote Sensing Sensors." *The GEOSS Era: Towards Operational Environmental Monitoring,* Sydney, Australia: 34th International

Symposium on Remote Sensing, http://www.isprs.org/proceedings/2011/isrse-34/211104015Final00252.pdf

APPENDIX

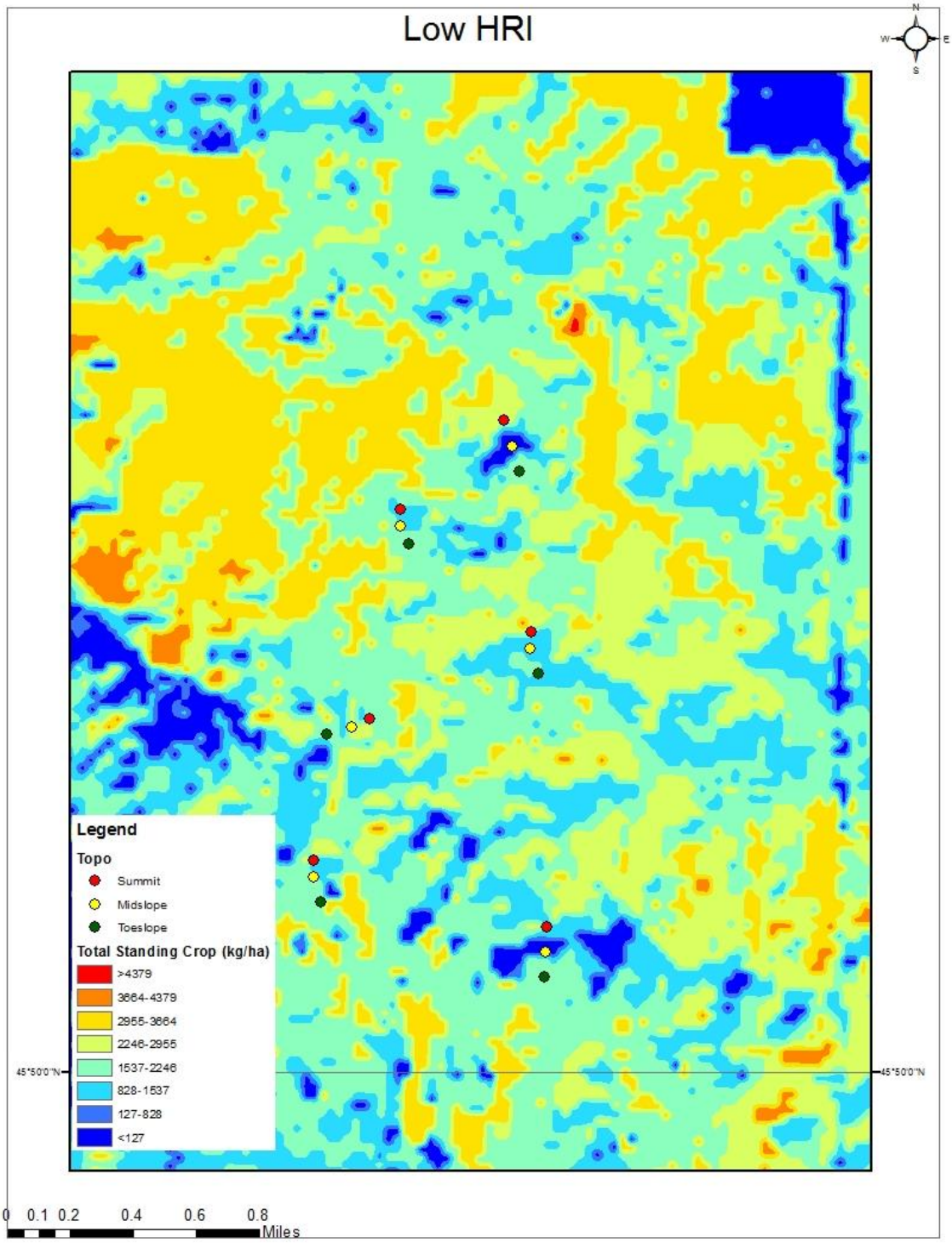

Figure 23. Site plot summit, midslope, and toeslope in four field sites in Low HRI within this map are located in Figure 3 Legend.

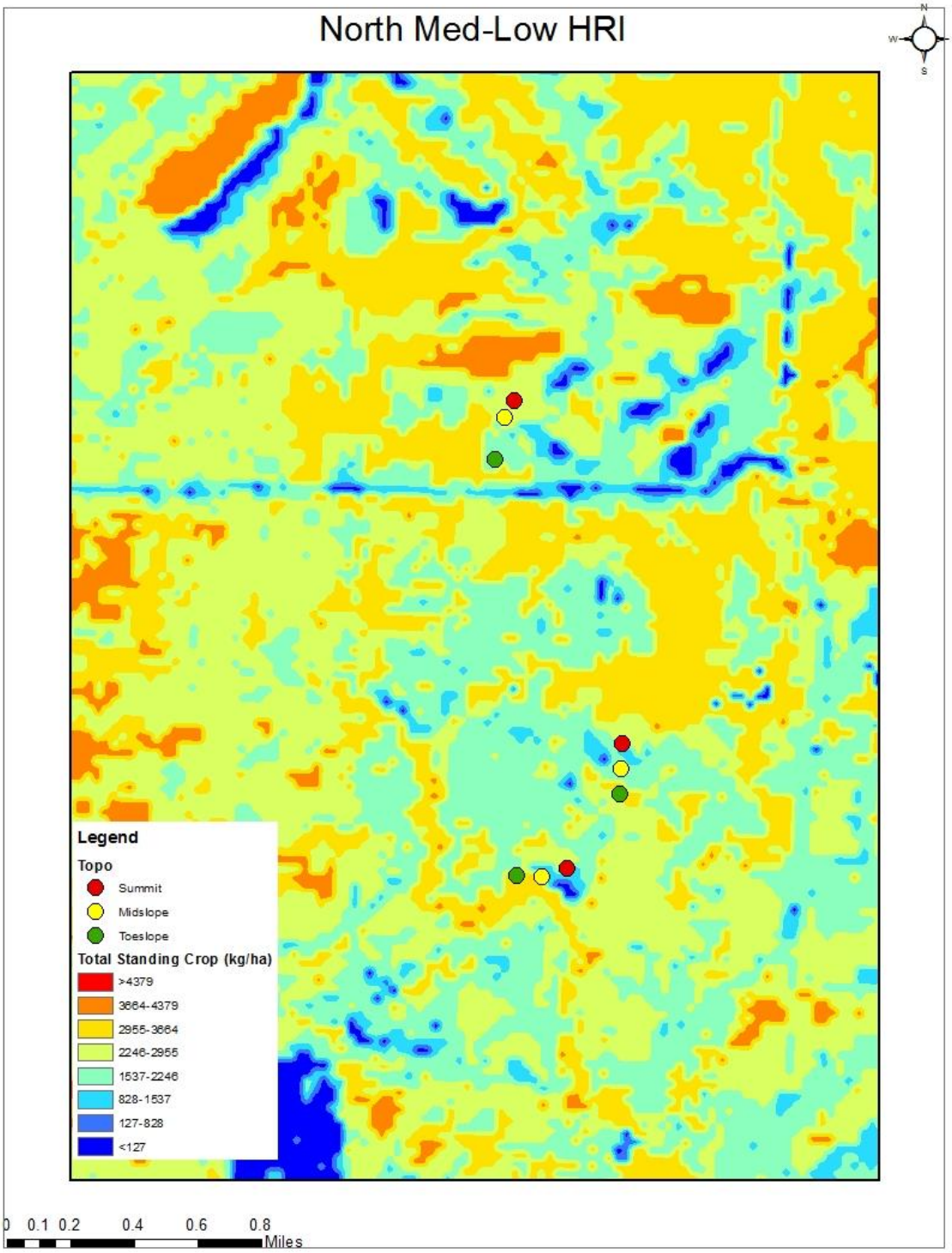

Figure 24. Site plot summit, midslope, and toeslope in two field sites in North Med-Low HRI within this map are located in Figure 3 Legend.

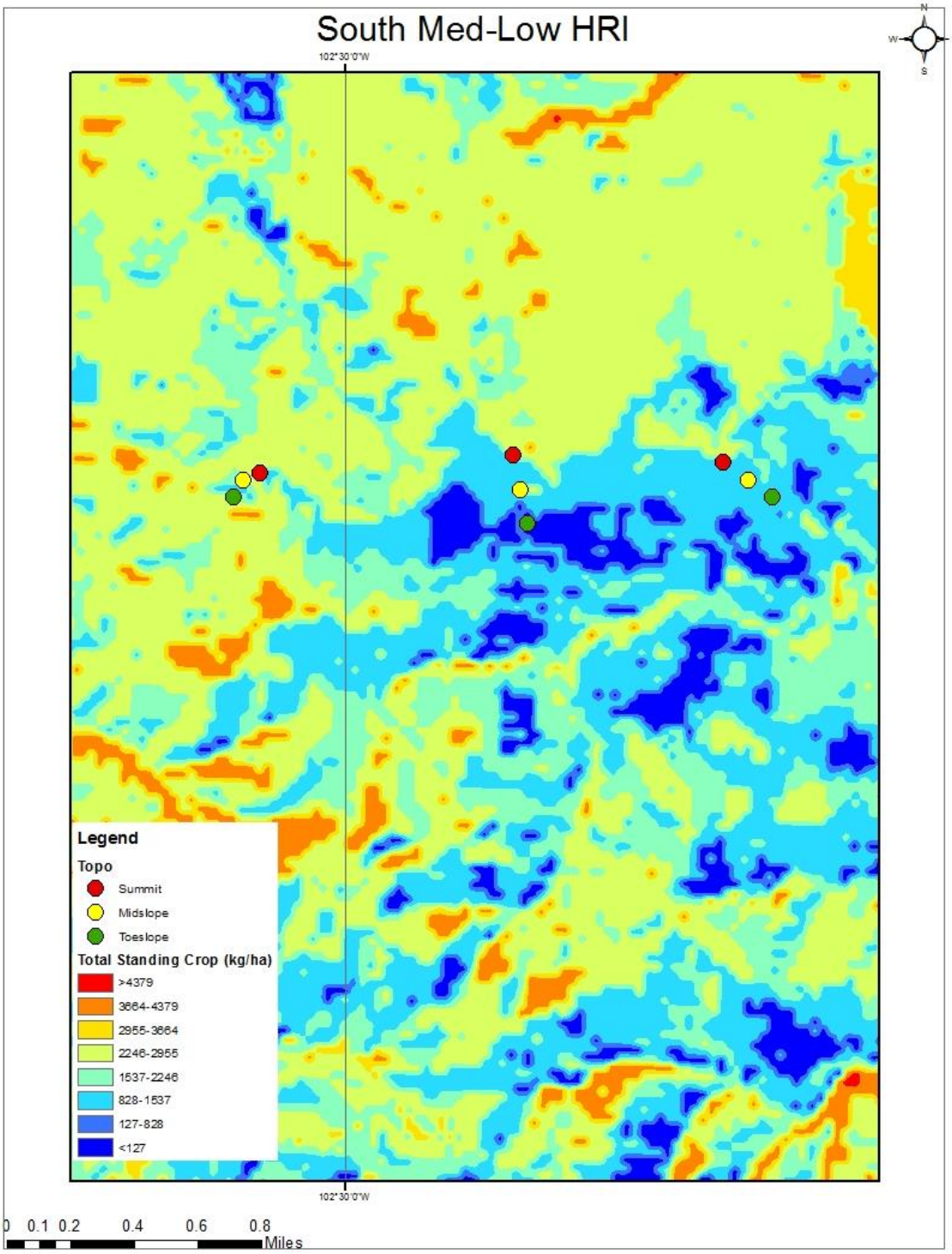

Figure 25. Site plot summit, midslope, and toeslope in three field sites in South Med-Low HRI within this map are located in Figure 3 Legend.

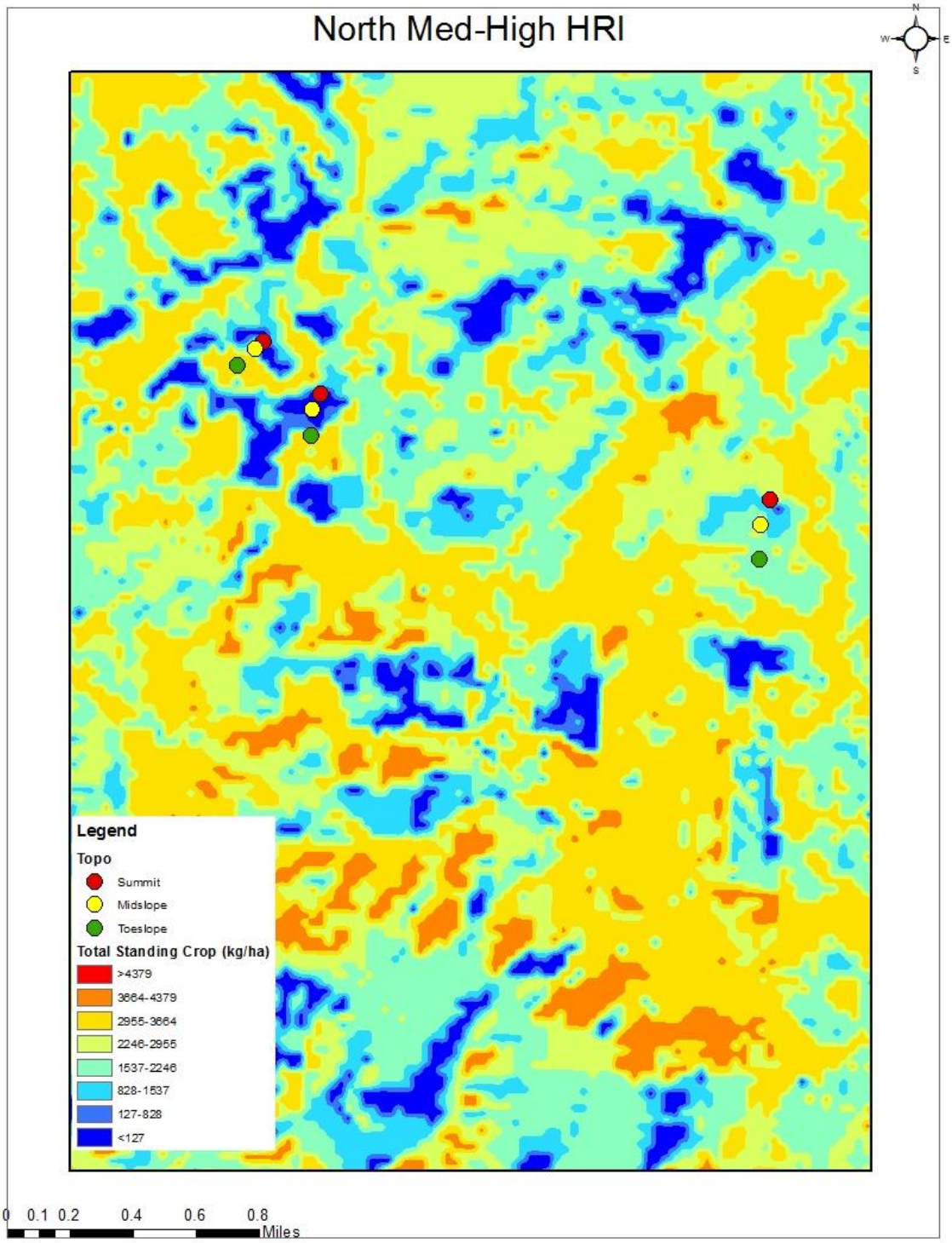

Figure 26. Site plot summit, midslope, and toeslope in three field sites in North Med-High HRI within this map are located in Figure 3 Legend.

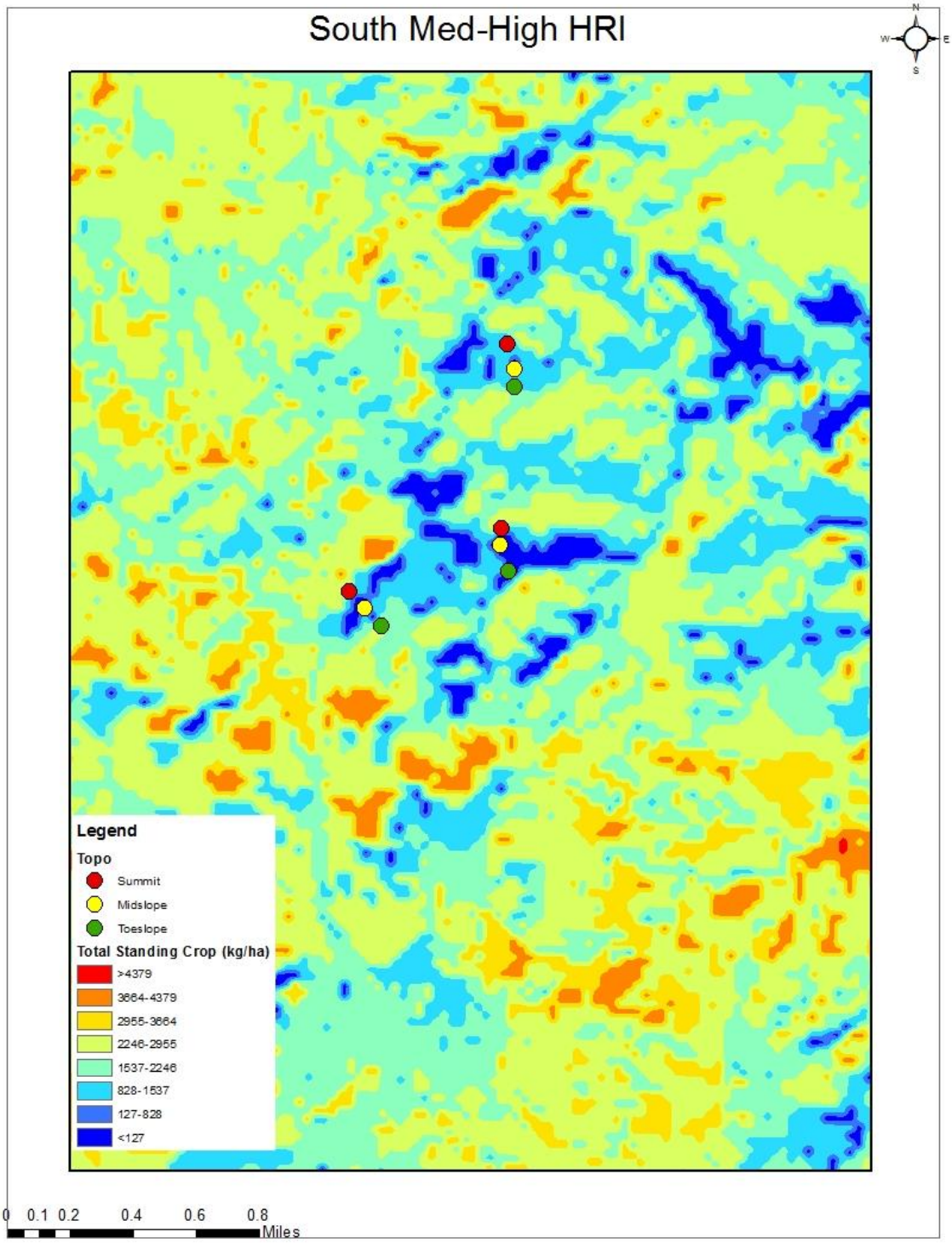

Figure 27. Site plot summit, midslope, and toeslope in six field sites in South Med-High HRI within this map are located in Figure 3 Legend.

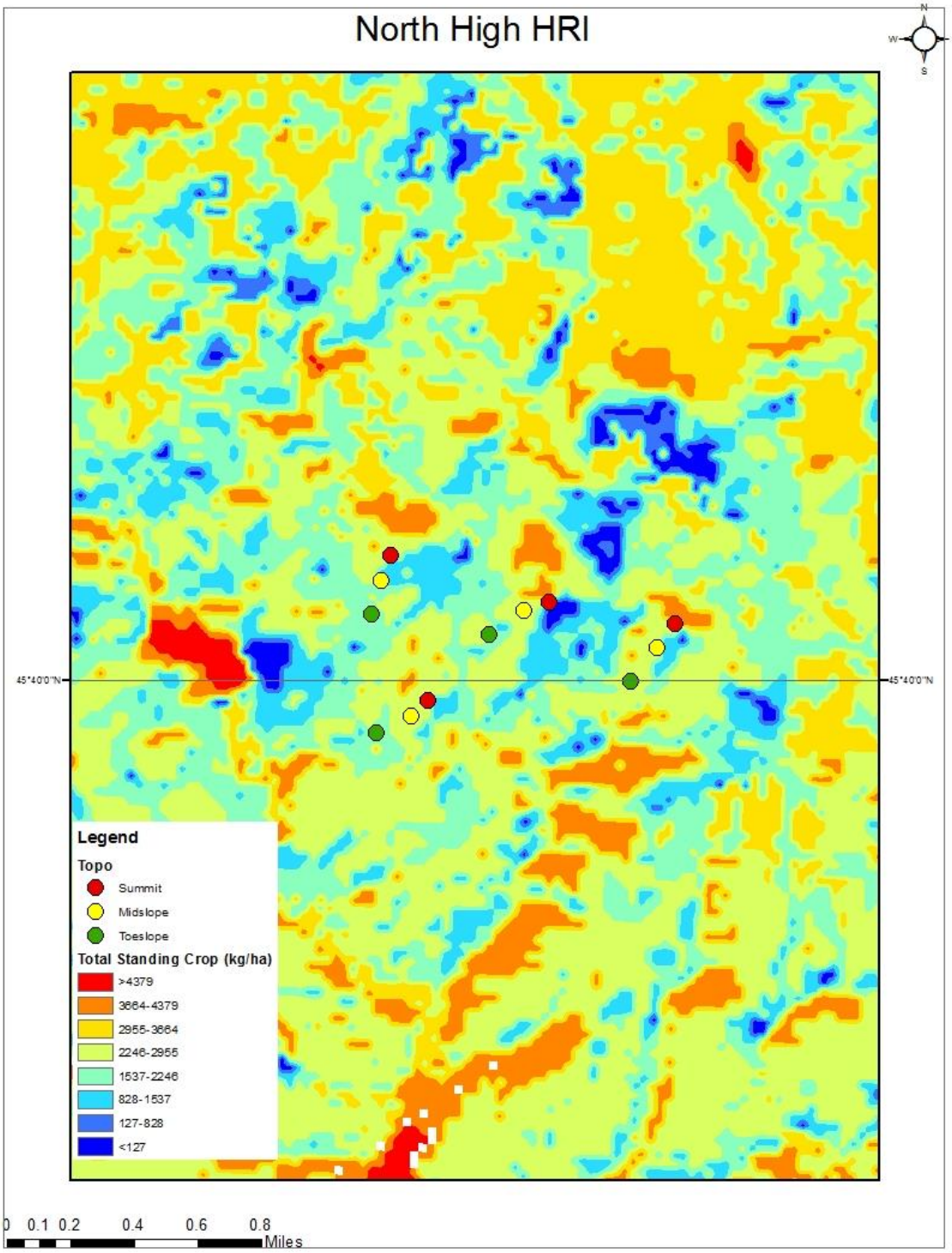

Figure 28. Site plot summit, midslope, and toeslope in three field sites in North High HRI within this map are located in Figure 3 Legend.

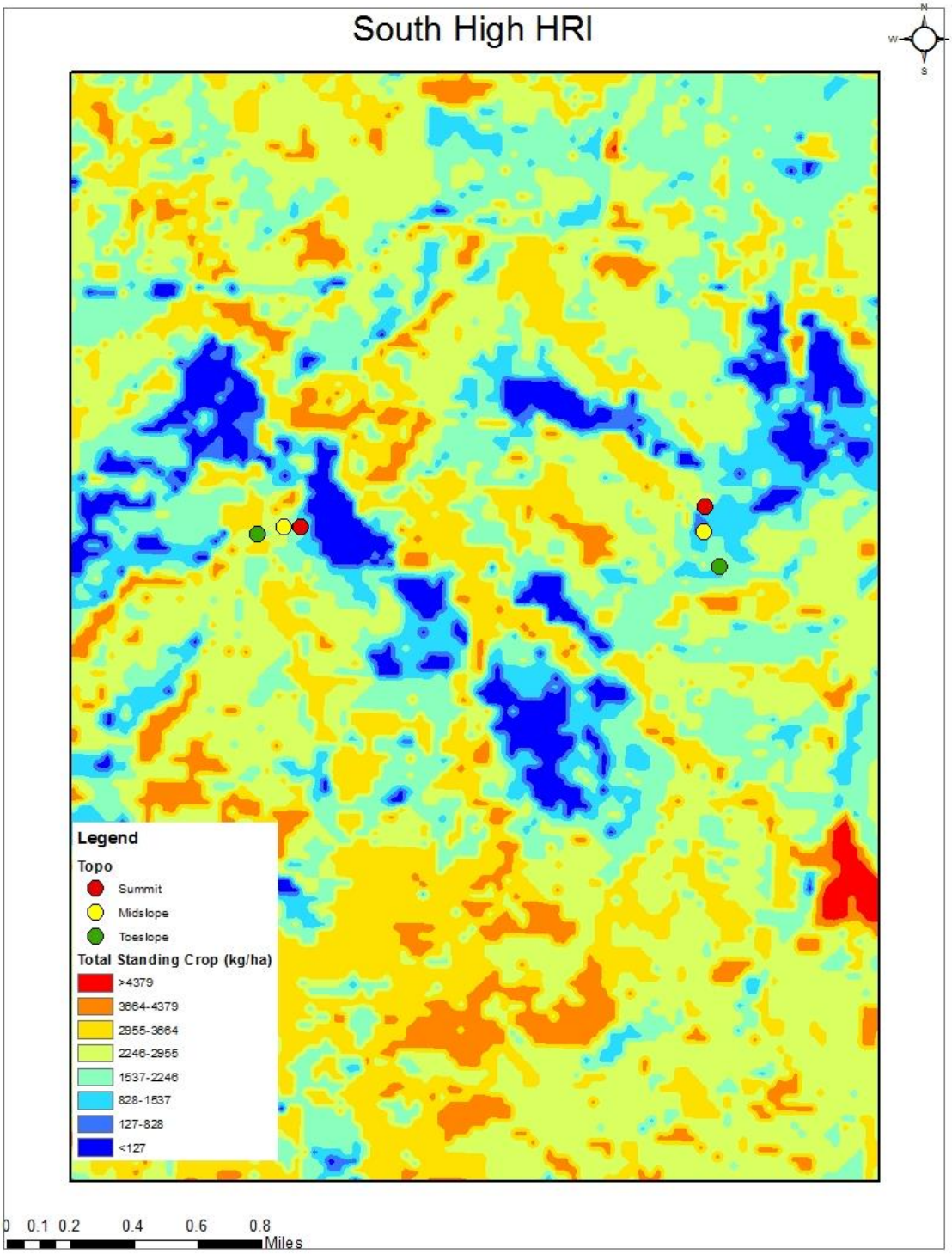

Figure 29. Site plot summit, midslope, and toeslope in three field sites in South High HRI within this map are located in Figure 3 Legend.